Self-Assembly of Colloidal Particles for Fabrication of Structural Color Materials toward Advanced Intelligent Systems

Heng Zhang, Xiuming Bu, SenPo Yip, Xiaoguang Liang, and Johnny C. Ho*

Inspired by the intelligent systems in nature, artificial systems with complicated practical functions have been developed for decades. The pathway toward the target is now based on the discoveries for new stimuli-responsive and free-standing materials to construct the advanced intelligent systems, instead of just electronic machines. Structural color materials, including both photonic crystalline and amorphous structures, are typical candidates due to the smart biomimetic characteristics, such as self-healing, autonomous regulation, and on-demand adaptability. However, to improve the stability and simplify the fabrication process of such materials, great efforts have been made in the modification of colloidal self-assembly techniques for more efficient real-life applications. A comprehensive review investigating various direct self-assembly techniques of colloids for the facile fabrication of structural color materials toward practical applications is provided. Recent advances of these self-assembly schemes of colloidal particles are presented, along with valuable design guidelines of these techniques to achieve efficient structural color materials for advanced intelligent systems.

1. Introduction

Intelligence of a system is the ability to sense the environment, store and analyze information, and respond accordingly.[1] Being inspired by nature, man-made electronic systems have also been demonstrated as intelligent systems.[2] Similarly, these systems are composed of many fundamental smart electronic components, such as logic gates and transistors. By controlling current flow, amplifying current,[3] and performing logical operations,[4] the integration of these individual parts has resulted in highly complicated analytical machines, namely, computers. On the basis of these electronic systems, the pathway to intelligence has been built by humans. However, one of the problems is that these electronic machines cannot operate without a constant power supply. As materials have to be freestanding, many types of applications (e.g., biomedical) will not be achieved if not tethered to an external power supply. That is why a piece of free-standing material (e.g., metallic, inorganic, or polymeric) is commonly regarded as static and passive. To create such smart materials, one possible approach is the use of stimuli-responsive materials.[2] By definition, these materials have the ability to sense their surroundings and produce a simple and direct response. More specifically, stimuli responsiveness is the capability of detecting a signal which is applied in the long distance or sensing a chemical substance that is occurring naturally. Signals being applied remotely involve changes in the surrounding like temperature, pressure, electric field, or magnetic field. Chemicals occurring naturally cover species found in minerals or produced by biological organisms. Synthetic molecules unavailable naturally are not regarded as stimuli. In this regard, having been studied for decades, a wide range of stimuli-responsive materials that can respond to many different types of stimuli has been fabricated. Among them, structural color materials are promising candidates for further intelligent applications.[5]

H. Zhang, X. Bu, Dr. S. P. Yip, Prof. J. C. Ho
Department of Materials Science and Engineering
City University of Hong Kong
Kowloon, Hong Kong
E-mail: johnnyho@cityu.edu.hk

H. Zhang, Dr. S. P. Yip, Prof. J. C. Ho
State Key Laboratory of Terahertz and Millimeter Waves
City University of Hong Kong
Kowloon, Hong Kong

The ORCID identification number(s) for the author(s) of this article can be found under https://doi.org/10.1002/aisy.201900085.

H. Zhang, Dr. S. P. Yip, Prof. J. C. Ho
Shenzhen Research Institute
City University of Hong Kong
Shenzhen 518057, P. R. China

Dr. X. Liang
Department of Physics
Guangxi Normal University
Guilin, Guangxi 541000, P. R. China

Prof. J. C. Ho
Centre for Functional Photonics
City University of Hong Kong
Kowloon, Hong Kong

**ADVANCED
SCIENCE NEWS**
www.advancedsciencenews.com

**ADVANCED
INTELLIGENT
SYSTEMS**
Open Access
www.advintellsyst.com

To deal with structural color materials, we have to know more about structural color. In contrast to pigmentary coloration, structural color is a type of coloration arising from visible light interference with certain structural features at the micro- or nanoscale. The former color is obtained from the physical properties of light, whereas the latter one involves energy consumption and conversion between light and electrons.[6,7] Structural coloration, dating back from the Cambrian explosion, is widely spread in natural creatures, which contributes to camouflage, reproduction, signal transmission, and so on.[8] Through bottom-up techniques, including controlled self-assembly, and top-down processing methods, like lithography, structural color materials can be fabricated and find applications in a large number of fields. For example, synthetic-responsive structural color materials have attracted remarkable interest because they can allow modulation of the colors for on-demand applications containing sensors, displays, anti-counterfeiting, smart devices, and others.[9] Moreover, self-regulating materials with autonomous color regulation capacity have been fabricated very recently, which shed light on next-generation photonic devices.[10] Other important features, such as self-healing and shaping memory, are on the way for more practical applications, even they are still in the experimental phase due to the huge difficulty of obtaining these materials.[11] Top-down and bottom-up methods are generally two main processing principles discovered by scientists until now. First, the top-down approaches on bulk material substrates attempt to use microfabrication tools like electron beam lithography to "sculpt" or "write" nanostructure patterns by computer designs. Lots of high-quality materials with photonic nanostructures have been successfully prepared via this method. However, with the limit of lithography, more complex structures, especially 3D fabrication, cannot be achieved. In addition, higher manufacturing cost and lower production efficiency hinder the large-scale production of advanced photonic materials. That is why the second type, bottom-up approaches, is more popular by building hierarchical ordered structures through self-assembly between basic building units, including molecular parts like block copolymers or liquid crystal molecules, and colloidal nanoparticles (NPs) such as submicron silica or polystyrene (PS) beads. Among these, assembly from colloidal units is the most favorable method being intensively investigated.[12,13] These colloidal particles to assemble like nanostructured materials (at least one of three dimensions is in the 1–100 nm range) possess a huge potential to be applicable and improve performance in advanced intelligent systems due to their quantum confinement effect, surface effect, nonlinear optical effect, and dielectric confinement effect.[14,15] Also, due to the versatility and capability of direct self-assembly techniques of colloids[16], we would perform a comprehensive review here to discuss about the recent advances of assembled colloidal particles to achieve efficient color change materials for the utilizations of various advanced intelligent systems.

Heng Zhang received her B.S. and M.S. degrees from the University of Science and Technology of China in 2012 and City University of Hong Kong in 2016, respectively. Currently, she is pursuing a Ph.D. degree under the supervision of Professor Johnny C. Ho in the Department of Materials Science and Engineering at City University of Hong Kong. Her research interests are nanostructured arrays fabricated by the Langmuir–Blodgett method and semiconductor nanowires in the applications of infrared and terahertz detectors.

Xiuming Bu received his M.S. degree from the School of Materials Science and Engineering, University of Shanghai for Science and Technology, P. R. China, in 2017. Currently, he is a Ph.D. student under the supervision of Professor Johnny C. Ho in the Department of Materials Science and Engineering at City University of Hong Kong. His research interests are the fabrication of nanomaterials and their applications in electronics and energy conversion.

Johnny C. Ho received his B.S. with high honors in chemical engineering in 2002 and his M.S. and Ph.D. in materials science and engineering from the University of California, Berkeley, in 2005 and 2009, respectively. From 2009 to 2010, he worked as a postdoctoral research fellow in the nanoscale synthesis and characterization group at Lawrence Livermore National Laboratory, California. Currently, he is an associate professor of materials science and engineering at City University of Hong Kong. His research interests focus on synthesis, characterization, integration, and device applications of nanoscale materials for various technological applications, including nanoelectronics, sensors, and energy harvesting.

include the hydrogen bonding interaction,[17] electrostatic interaction,[18] hydrophilic and hydrophobic effect,[19] charge compensation effect,[20] and capillary action. During the past decades, the direct self-assembly of colloidal particles has been widely utilized to fabricate numerous hierarchical and periodic micro-/nanostructure arrays in a large scale, owing to the cost-effectiveness, simple processing, high throughput, and excellent controllability.[21–23] In this section, we will summarize the recent progress based on typical self-assembly methods with colloidal microspheres or NPs, such as PS particles, silica NPs, and Au NPs.

2. Direct Self-Assembly of Colloids

Having been developed since the early 1950s, the direct self-assembly of microspheres refers to the close packing or orderly arranging of microspheres under the action of a driving force.[16] More specifically, the driving force between microspheres can

2.1. Evaporation-Induced Method

Surface evaporation-based self-assembly process was first discovered by Denkov et al., which is further often used for

1900085 (2 of 20)

ADVANCED
SCIENCE NEWS
www.advancedsciencenews.com

ADVANCED
INTELLIGENT
SYSTEMS
Open Access
www.advintellsyst.com

the preparation of colloid crystals. The preparation principle is to add certain concentration of colloidal suspension onto a clean substrate surface or conversely insert the substrate into colloidal suspension medium. During the formation process, it has been proposed that the array ordering begins when the thickness of the solvent layer becomes approximately equal to the particle diameter. Also, the solvent evaporation rate and the shape of the surface affect considerably the quality of the obtained arrays.[24] In addition, neither the electrostatic repulsion nor the van der Waals attraction between the particles is responsible for the formation of 2D crystals. The illustrative stress diagram of the horizontal and vertical evaporation process is shown in **Figure 1**.[24,25] There are two basic ways of evaporation-induced processes, namely horizontal self-assembly and vertical self-assembly.

To improve the uniformity of the colloidal self-assembly, researchers have then developed new methods to fabricate micro-/NP clusters by applying evaporative self-assembly in picoliter-scale droplets of particle suspension onto a hydrophobic surface. The gravity force and the surface tension force of a contacting surface drive the formation of droplets from a nanofabricated printing head. By changing the concentration of particle suspension, they can prepare multiplex printing of various particle clusters, as shown in **Figure 2**.[26] The deposition morphology of inkjet printing is determined by the substrate wettability, the ink formulation, and the substrate temperature.[27]

2.2. Interface-Induced Method

Interface self-assembly, as one of the earliest proposed methods for preparing 2D or 3D colloidal crystals, has been achieved at the gas–liquid and liquid–liquid interface. On the gas–liquid interface, an ordered array would be formed after spreading colloid microsphere suspension onto the liquid surface. Then, the colloidal crystals are transferred to a clean substrate. The Langmuir–Blodgett (LB) technique, developed in the early 1930s, is one of the typical interface self-assembly trials successfully transferring the amphiphilic films spread out on the liquid surface to the substrate for the preparation of monolayer or multilayer films. The general working principle is quite simple and usually used with surfactants, such as oil. The colloids would spread as far as possible once a colloidal suspension is dispersed onto a surface and then form a monolayer. Afterward, the film is compressed by a barrier, reducing the available surface area and resulting in an
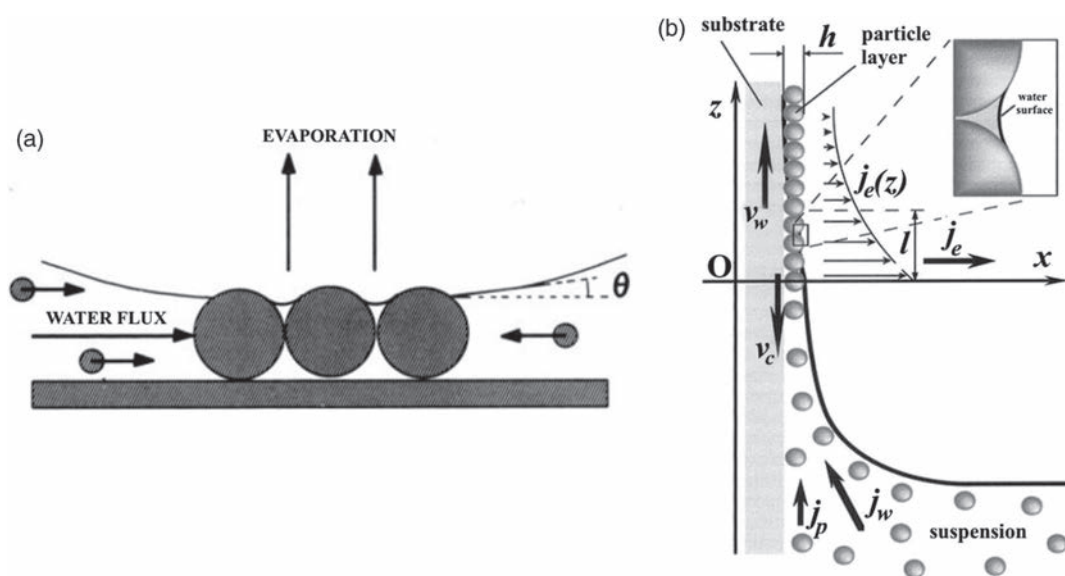

Figure 1. The illustrative diagram of the evaporation-induced a) horizontal and b) vertical self-assembly in 2D colloidal array. a) Reproduced with permission.[24] Copyright 1992, American Chemical Society. b) Vertical self-assembly during the fabrication of monolayer microsphere array: v_w is the withdrawal rate of the substrate, v_c is the formation speed of the crystals, j_w is the water influx, j_p and j_e are the particle influx and the water evaporation flux, respectively, and h is the thickness of the array. Reproduced with permission.[25] Copyright 1996, American Chemical Society.
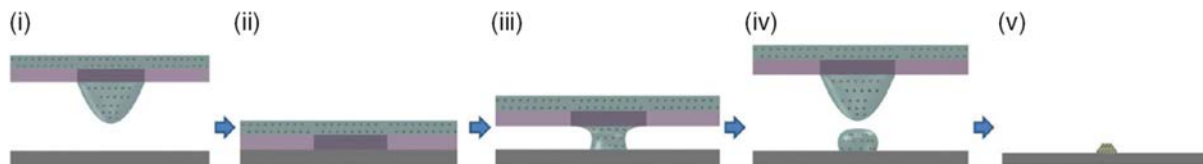

Figure 2. Diagram of the printing procedure in serial processes. (i) Particle suspension menisci are extruded by the influence of gravity. (ii) Contacting of the particle suspension menisci with the substrate. (iii) Surface tension of the substrate attracts a fraction of the suspension fluid. (iv) Picoliter-scale droplets are transferred to the substrate via pinch-off processes. (v) Rapid evaporative self-assembly of the particles for the fabrication of 3D clusters. Reproduced with permission.[26] Copyright 2012, American Chemical Society.

**ADVANCED
SCIENCE NEWS**

www.advancedsciencenews.com

**ADVANCED
INTELLIGENT
SYSTEMS**
Open Access

www.advintellsyst.com

increased surface tension.[28] In the transfer process, a substrate is "scooped" through this compressed film, whereas the lower surface tension provided by the substrate would subsequently cause the colloids to transfer onto it from the interface. In this method, the colloidal NPs (e.g., silica and PS nanospheres) are usually used to form self-assembled monolayers with the hydrophobic surface, as shown in **Figure 3**.[29] Also, the LB technique was further improved by a surfactant-free LB technique by Ruan and co-workers.[30]

In the meantime, a liquid–liquid self-assembly method was also developed. Reduction in interfacial energy gives a driving force to assemble the particles at the interface, and lateral interface-mediated capillary forces of various origins can further control the assembly process, as shown in **Figure 4**.[31] Especially for the nonspherical particles dressed with particular ligands, this has proven to be a universal tool for assembly. Even NPs can become essentially irreversibly trapped at interfaces, particularly with larger-sized particles being driven most effectively to the interface. This phenomenon has been shown for specifically coated CdSe NPs.[32] Different orientation and packing structures of nanorods at the liquid–liquid interface can hence be generated by controlling the aspect ratio, surface properties, concentration, and solvent evaporation rates.[33] Isa et al. fabricated nonclose-packed particle arrays, where the separation can be controlled between 3 and 10 particle diameters. The smallest size of these colloidal particles could be controlled down to 40 nm, as shown in **Figure 5**.[31]

2.3. Template-Assisted Method

Geometrically, templates can be defined as substrates (in 1D, 2D, or 3D) with modified surface-containing active sites, which can selectively induce NP deposition. Recently, those templates can be divided into soft and hard templates.[34] In polymer science, soft templates, such as single molecules,[35] microstructures (e.g., carbon nanotubes),[36] or block copolymers,[37] possess a spatial distribution of specific reactive sites and often serve as scaffolds arranging different particles into aimed structures (e.g., DNA) with morphologies complementary to that of the templates. Compared with soft templates, physical hard templates can be fabricated with higher accuracy using photolithography,
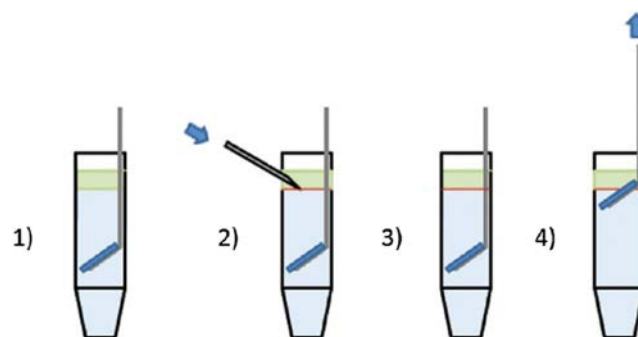
Figure 4. Schematic diagram of the colloidal self-assembly procedure at liquid–liquid interfaces. Reproduced with permission.[31] Copyright 2010, American Chemical Society.

reactive ion etching, electronic etching, focused ion beam (FIB) etching, and other ways of etching. To get the colloidal self-assembly, template methods are commonly combined with other techniques like evaporation, convection capillary force, spin-coating process, and so on.[38–41] Kim et al. have demonstrated recently high-resolution light-emitting diodes based on well-defined nanoarrays of colloidal quantum dots (QDs) with different sizes in a large area using nanoporous templates.[42] By combining soft lithography and template-assisted colloidal self-assembly, Gupta and co-workers have fabricated a stretchable periodic square lattice of gold NPs on macroscopic areas obtaining mechanically tunable, cost-efficient, and low-loss plasmonic nanostructures that show pronounced optical anisotropy upon mechanical deformation.[43]

At the same time, Xu and co-workers have used FIB to fabricate nanohole arrays as templates for the self-assembly of PS microspheres, as shown in **Figure 6**.[44] Further with the help of capillary force, Yin and co-workers made a series of explorations to improve physical template self-assembly method to assemble monodispersed spherical colloids on complex patterned templates, including polygonal or polyhedral clusters, linear or zigzag chains, and circular rings, fabricated by photolithography, as shown in **Figure 7**.[45–48] The capillary force has been found to be strong enough to induce a preferential orientation in the plane of the solid substrate.
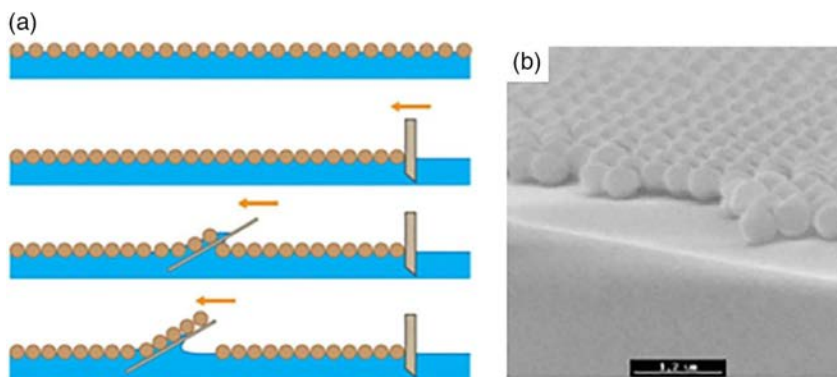
Figure 3. Fluidic deposition: Langmuir–Blodgett method. a) Schematic drawing of the method. b) Scanning electron microscopy (SEM) images of a monolayer of colloidal crystals. Reproduced with permission.[29] Copyright 2018, Elsevier.
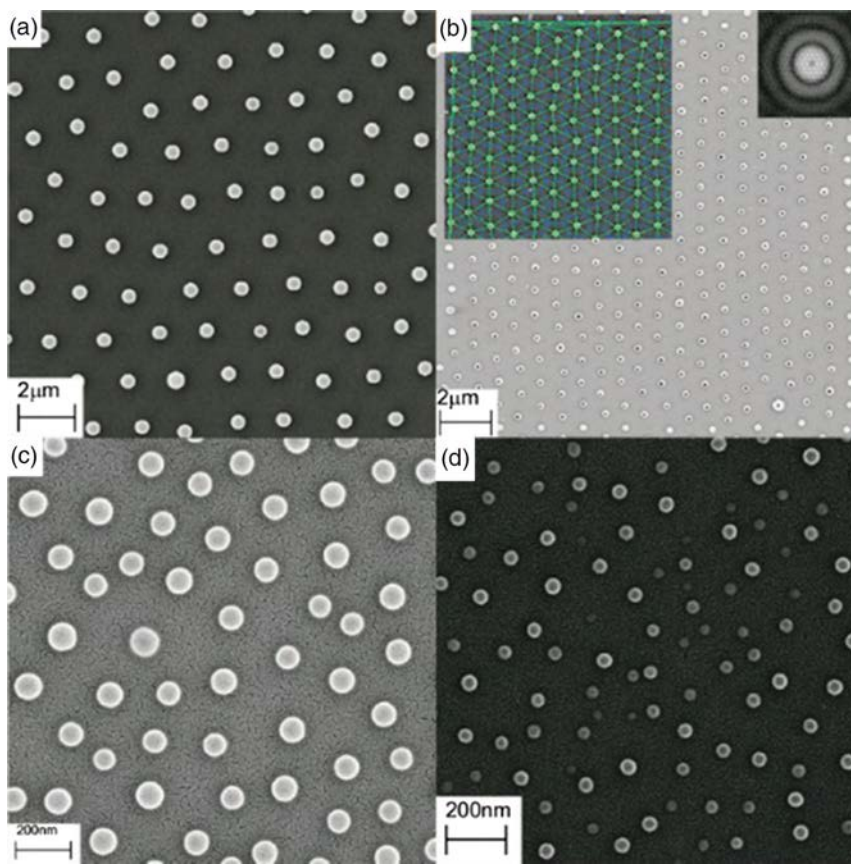
1900085 (4 of 20)

Figure 5. SEM images of amidine latex PS arrays produced on SiO_2 with different diameters in average: a) 500 nm, b) 200 nm, c) 100 nm, and d) 40 nm. Reproduced with permission.[31] Copyright 2010, American Chemical Society.
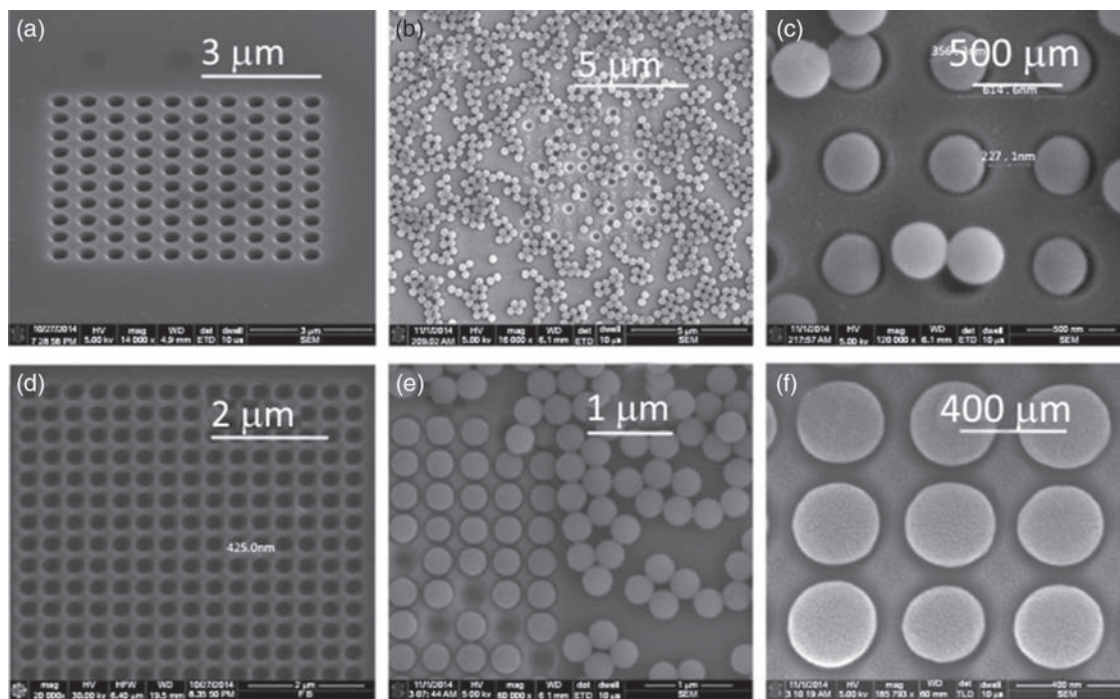

Figure 6. a–f) SEM images of surface-enhanced Raman scattering substrates with different sizes by FIB nanopatterning regulation and subsequent PS microspheres self-assembling, respectively. Reproduced with permission.[44] Copyright 2015, Elsevier.
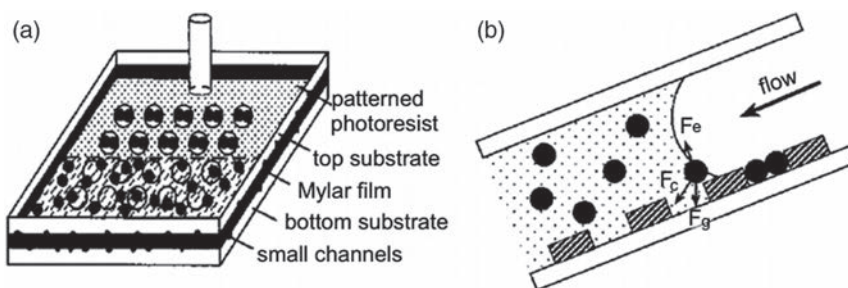
**ADVANCED
SCIENCE NEWS**
www.advancedsciencenews.com

**ADVANCED
INTELLIGENT
SYSTEMS**
Open Access
www.advintellsyst.com

Figure 7. a) Schematic diagram of template colloidal self-assembly combined with convection capillary force. b) The stress diagram of particles when they are on the rear edge of the liquid slug. Fc: capillary force, Fg: gravitational force, and Fe: electrostatic force. Reproduced with permission.[49] Copyright 2001, American Chemical Society.

2.4. External Physical Fields-Induced Method

External physical fields have long been a powerful means to control particle suspensions for the use of tailoring the mechanical, optical, and electronic properties of materials in applications of electromechanical systems and electronic inks. More recently, external fields have become the essential methods to direct the assembly of colloidal particles and NPs. Obviously, electric or magnetic fields are potential candidates for the field-directed assembly. For these reasons, field-directed assembly is demonstrated to be a key paradigm in the bottom-up fabrication of novel functional nanostructures which would enable the brand new materials and devices.

Under the effect of electric and magnetic fields, colloidal assembly occurs because of the induced interactions. Studies of mechanisms in such field-induced interactions in suspensions have been reviewed in great detail for both electrically and magnetically and polarizable colloids.[50] To be specific, most particles will polarize in electric fields as their dielectric properties mismatch with the surrounding medium.[51] Mobile charges, for example, those in an electrostatic double layer, also respond to applied fields and can also contribute to the polarization.[52] The induced field surrounding a polarized particle would form a dipole and then lead to a strong, anisotropic dipole–dipole interaction between particles in the far field. Furthermore, particles come into being dipolar chains at the time the interaction is strong to overcome Brownian motion; therefore, over longer times, they coarsen as chains laterally coalesce. In the ideal condition, the coarsening can proceed indefinitely to form the lowest energy structure, a body-centered tetragonal (bct), hexagonal close-packed (hcp), or face-centered cubic (fcc) lattice, according to the particle concentration and field which exist in the surrounding.[53–55] But in reality, kinetically jammed states of percolated chains often prevent this from happening due to interaction energies that are significantly greater than the thermal energy (kT), which is the typical mechanism in the self-assembly of electrorheological and magnetorheological fluids.[56] Some representative examples using this method are shown in **Figure 8**. More thorough studies of external physical fields have been explored in recent research. Sherman et al. have developed a complete thermodynamic description of assemblies for spherical NPs polarizing in

response to an externally applied electric or magnetic field.[57] Colla et al. also have come up with a coarse-grained description, in which effective interactions among the charged microgels are induced by both equilibrium ionic distributions and their time-averaged hydrodynamic responses to the applied electric field.[58]

2.5. Chemical Stimuli-Induced Method

Inspired by those ideas developed in polymer science or supramolecular chemistry,[60,61] chemistry is considered as a potential powerful handle toward creating ordered assemblies through molecular interactions. Recent achievements in this area have focused on designing particles with stimuli-responsive interparticle interactions and morphological or functional features that result in directional interactions. Grzelczak et al. have reviewed diverse stimuli that have successfully been used to direct reversible NP self-assembly, including solvents, acid/base signals, metal ions, gases, biomacromolecules, and redox signals.[62] Ligand-protected gold NPs are particularly attractive for being extensively used over the last decade as building blocks in constructing superlattices or dynamic aggregates. Usually in most of the colloid systems, the noncovalent interactions including hydrophobic interaction, hydrogen bonding, electrostatic interactions, π–π stacking interactions, and so on exist. Hence, self-assembly acts as an important and effective strategy for bottom-up nanotechnology by organizing various well-defined building blocks into complex architectures through noncovalent interactions which has been adopted in the construction of the 1D–3D architectures.[63,64] Typically for the electrostatic interactions, long-range interactions between charged particles in aqueous systems can drive the self-assembly of the particles in an isotropic crystallization mode, such as 1D nanochains. One characteristic example is the assembly of gold NPs widely investigated in the surface plasmon resonance (SPR) properties. Long-range electrostatic repulsion forces are observed to control the growth of charged Au NP chains forming Au chain-like nanostructures.[65] Based on this, Yin et al. have obtained the first silica-coated Au nanochains with different NP size via the self-assembly process. Moreover, the SPR properties of Au nanochains can be easily tuned during the assembly process, as shown in **Figure 9**.[66]
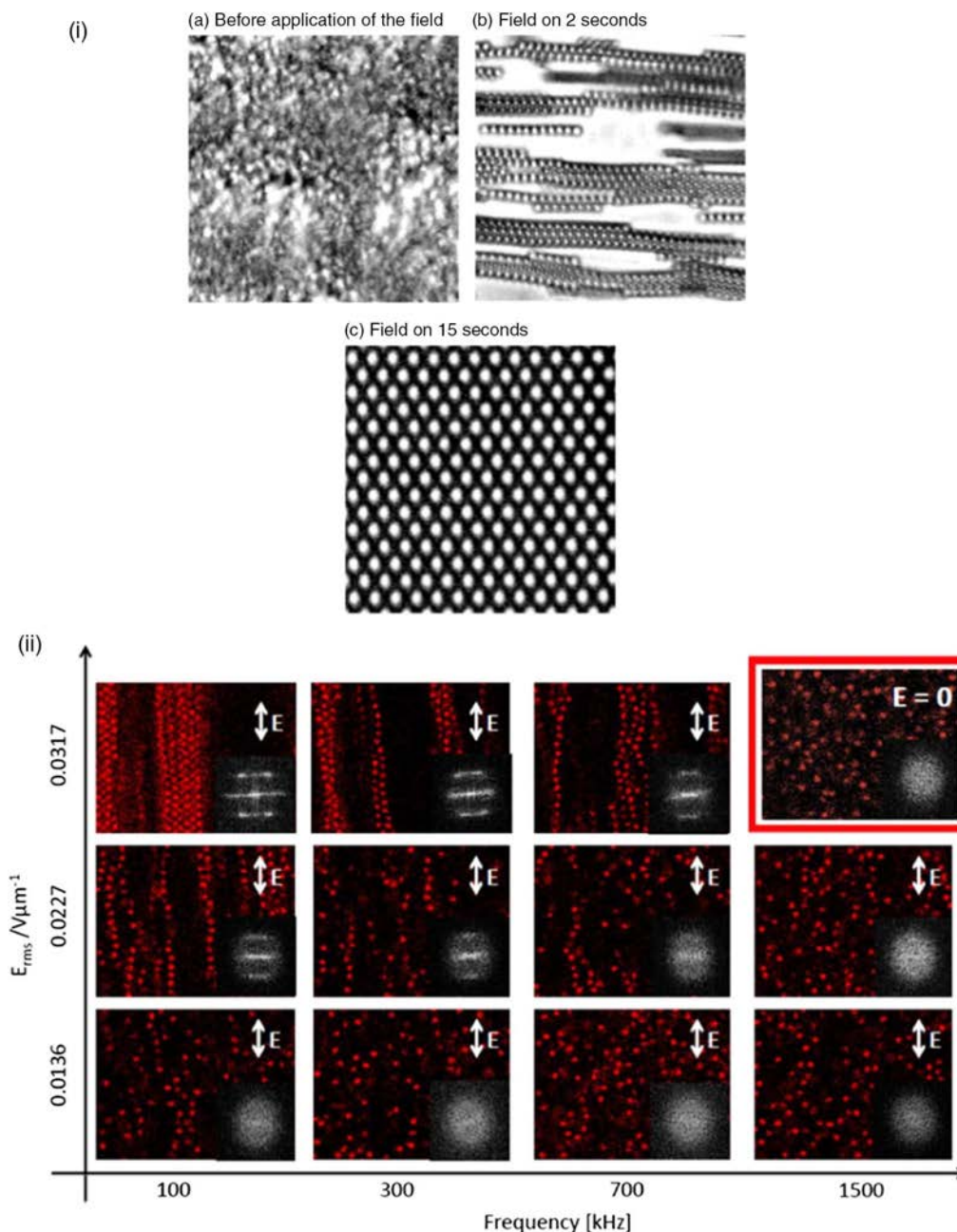
1900085 (6 of 20)

Figure 8. Directed assembly of particles in external fields (i) including assembly of micrometer-diameter colloidal particles into hcp arrays in AC electric fields. Reproduced with permission.[59] Copyright 2004, American Chemical Society. (ii) Confocal laser scanning microscopy images of field-driven self-assembly of ionic microgels at an effective volume fraction of $\phi_{eff} = 0.1$ in the swollen state ($T = 20\,°C$) as a function of field strength Erms and frequency f. Shown are 2D snapshots and an inset that depicts the Fourier transform of the corresponding image. Also shown is an image obtained with the suspension at zero field in the upper-right corner. Reproduced with permission.[58] Copyright 2018, American Chemical Society.

3. Fabrication of Structural Color Materials by Colloidal Assembly

As a widespread phenomenon in natural creatures contributing to camouflage, reproduction, signal transmission, and so on, structural coloration can be traced back from the Cambrian explosion.[67] Structural color is a type of coloration which is caused by visible light interference with certain structural features at the micro- or nanoscale.[68] Different from pigmentary coloration which originates from the physical properties of light, structural color results from energy consumption and conversion between light and electrons.[69] Hook and Newton began the earliest scientific studies of structural coloration in the 17th century, followed up by series of researchers more directly observing the
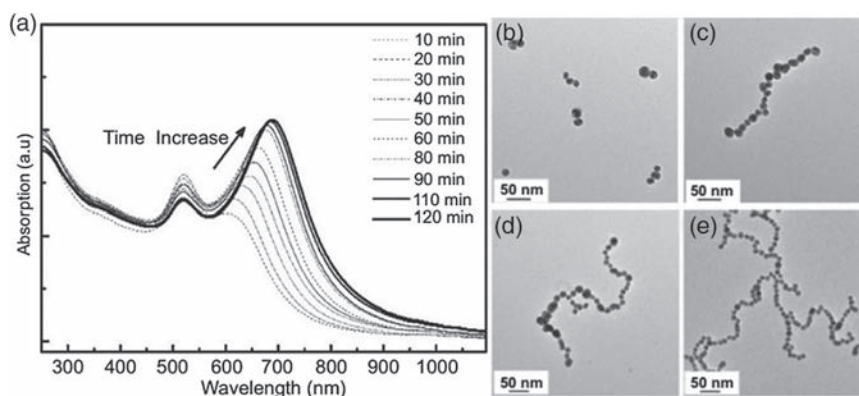
ADVANCED
SCIENCE NEWS

www.advancedsciencenews.com

ADVANCED
INTELLIGENT
SYSTEMS
Open Access

www.advintellsyst.com

Figure 9. a) UV–vis spectra evolution of the Au_{13} NPs solution after addition of ammonia water during the self-assembly process. Typical transmission electron microscopy (TEM) images of the assemblies at different stages: b) 10 min; c) 40 min; d) 60 min, and e) 120 min. Reproduced with permission.[66] Copyright 2014, WILEY-VCH Verlag GmbH & Co. KGaA, Weinheim.

nanostructures via electron microscopy and establishing electromagnetic theories step by step.[70] In practice, this definite explanation of the relationship between structure and coloration offers the principle for on-demand materials design at the nanoscale. Moreover, due to their special colors, they have been found in applications of decoration, printing, and displays.[71] Other than this, they can also function as light wave-guiding components for photonic communication and integrated optoelectronic systems.[72,73] In addition, as they can be made stimuli responsive, sensors in anticounterfeiting and chemical/biomedical analysis would also be in need of these kinds of materials.[13,74]

To obtain more subtle and complex structures applicable in stimuli-responsive systems, the bottom-up self-assembly of colloidal particles discussed earlier, always combined with traditional top-down technologies, such as lithography, acts as a facile and cost-effective bottom-up strategy for fabrication of photonic materials. In this section, we will review the traditional and state-of-the-art self-assembly technologies for fabrication of 3D photonic materials used in structural colors with controllable long- and short-range orders.

3.1. Crystalline Colloidal Arrays

Photonic crystalline structures (PCSs) were first proven by Yablonovitch and John in 1987 to generate a photonic bandgap (PBG) from the point view of the electromagnetic field.[75,76] Light with a certain wavelength in the PBG is forbidden to propagate. A structural color is generated when the PBG of a PCS is in the visible region, as shown in **Figure 10**a.[77] The characteristic wavelengths of the diffracted light can be determined according to the following Bragg equation

$$m\lambda = 2nd \sin\theta \tag{1}$$

where m is the series of diffraction, λ is the wavelength of diffraction, n is the average refractive index (RI), d is the lattice constant, and θ is the angle between the incident light and the normal crystal plane.[78,79] Based on the theory provided by the above formula, any change in the parameters of the Bragg equation would affect the design and preparation of a
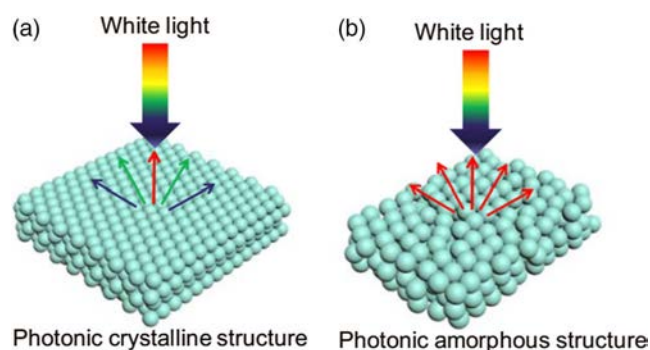

Figure 10. Typical photonic nanostructures of colloidal assembled structural colors: a) highly ordered PCSs generating iridescence and b) short-ordered PASs generating noniridescence. Reproduced with permission.[77] Copyright 2019, Royal Society of Chemistry.

modulated structural color material. For instance, the structural colors of PCSs change with the view or light incidence angle.[80]

To fabricate crystalline colloidal arrays, self-assembly of colloidal particles provides a facile and efficient route. It was first reported by Bogomolov et al.,[81] about the application of crystalline colloidal arrays to PCSs, and followed by Mayoral et al.[82] Since then, evaporation-induced colloidal assembly has been the most widely used method for producing structural colors with crystalline colloidal arrays. Early research about the colloidal assembly with periodic hexagonal arrays was inspired from evaporating solutions of polymers under a flow of moist gas.[83] Xia and co-workers have found a similar gas-flow force approach to assemble PS particles into 3D crystalline colloidal arrays.[84] In spite of being simple and practical, this method still needs conventional photolithography, which requires the availability of a liquid precursor that does not swell or dissolve the template. For improvement, Nagayama and co-workers developed the vertical deposition method using the solvent evaporation-assisted method to assemble PCSs under the interaction of capillary force and surface tension.[25] As described in the last section, PCSs can assemble on the substrate under the interaction of a capillary force and surface tension. Before long, Colvin's team has successfully used this method to fabricate large-area, highly ordered

**ADVANCED
SCIENCE NEWS**
www.advancedsciencenews.com

**ADVANCED
INTELLIGENT
SYSTEMS**
Open Access
www.advintellsyst.com

silica colloidal single-crystal films with good optical contrast and mechanical stability.[85] Through the vertical deposition method shown in **Figure 11**a,[86] not only a monolayer but multiple layers of ordered colloidal crystals can be prepared on a vertically placed substrate via the adjustment of temperature, humidity, concentration of colloidal solution, and growth time. However, to solve the problem of sedimentation of large particles in the vertical method, the methods of agitation, convection compensation, pulling, and flow control are proposed in the following research. For the agitation method, Ozin et al. present the magnetic stirring-assisted evaporation-induced self-assembly to avoid large-particle sedimentation in Figure 11b. A magnetic stirrer was placed at the bottom of the solution to avoid large-particle precipitation in the process of solvent evaporation.[87] In the convection compensation method, continuous convection is produced via the temperature gradient at the top and bottom of the container in the colloidal particles solution, thereby reducing the effect of large-particle sedimentation and obtaining a more uniform colloidal crystal film that had far fewer colloidal crystal defects than in gravity sedimentation.[88] Furthermore, a pulling approach like LB method shown in Figure 11c in a colloidal assembly can make up for the deficiency of relying solely on solvent evaporation.[89] The thickness of the colloidal crystal film can be controlled more accurately by changing the volume fraction of colloidal particles in the solution and the pulling speed of the motor. Therefore, a colloidal crystal film with higher quality and uniformity can be obtained as compared with the vertical method. As the substrate is pulling up rather faster than the evaporation rate of the solvent and the sedimentation rate of particles, this method can avoid the issue of the change in colloidal particle concentration during solvent evaporation. Particularly for the kind of charged colloidal NPs, field force-induced self-assembly is also

an effective approach for assembling monodispersed colloidal particles to form PCSs. Hence, an electrophoresis method has been discovered to prepare thick PCS films under the capillary electrophoresis effect in Figure 11d.[90] The particles were assembled into the PCS between the gaps by capillary force. The thickness of the film was tunable by controlling the liquid evaporation in the capillary cell using the electrophoresis effect. In addition, Gu and co-workers further developed a similar strategy for preparation of the inverse opal PCS structural color films using the electrophoresis effect illustrated.[86] Spin coating can also help prepare a closely packed colloidal film as the solvent flows through the substrate at a high shear rate in the process. By controlling the parameters of spin coating, an ordered PCS could be obtained. An experimental system has been built by Wu and co-workers to assemble PS particles of a size ranging from 223 to 1300 nm and form a close-packed colloidal crystal using spin-coating technology.[91] They have provided a very valuable reference for fabrication of large-scale and uniform PCS films with PS nanospheres of various diameters by spin-coating technologies.

In the methods based on evaporation of solvents, an increase in the volume fraction of the dispersed particles may be induced and cause more defects every 50–250 mm in solid colloidal crystal films. Therefore, to decrease the concentration of assembled colloidal particles, researchers have explored the liquid–gas method to fabricate free-standing colloidal crystal films.[92] This strategy can enable the creation of structural color films crack free over several square millimeters. Furthermore, the air/water/air interface would also provide a platform to control the dynamics of the colloidal self-assembly, which may have an enormous promise in photonic applications.

Apart from simple solvent evaporation methods, the template-assembled colloidal assembly with various patterns is also a
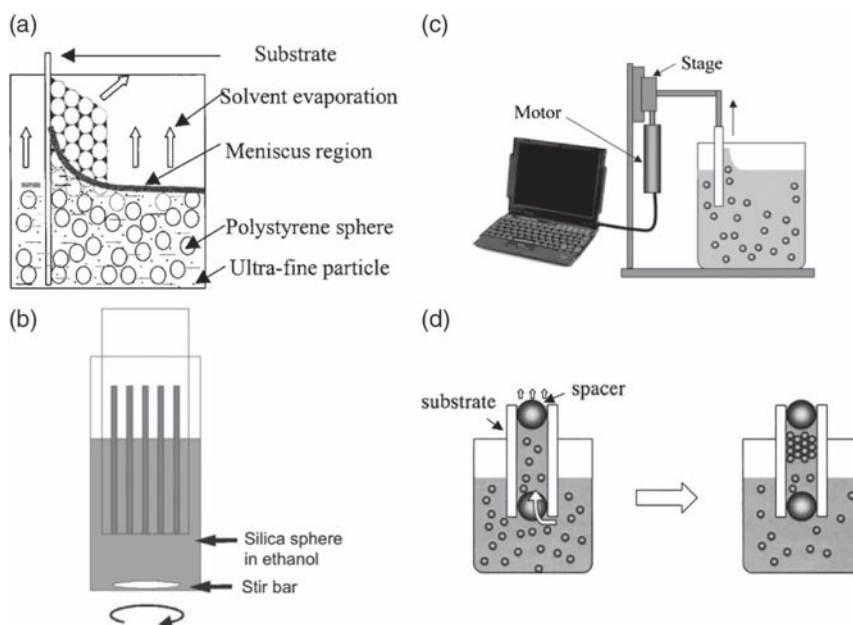

Figure 11. Schematic diagrams of a) the simple method of coassembly using general vertical deposition method. Reproduced with permission.[86] Copyright 2000, AIP Publishing. b) Magnetic stirring-assisted evaporation-induced self-assembly. Reproduced with permission.[87] Copyright 2000, WILEY-VCH Verlag GmbH & Co. KGaA, Weinheim. c) Pulling approach. Reproduced with permission.[89] Copyright 2002, American Chemical Society. d) Assembling monodispersed spheres between electrodes. Reproduced with permission.[90] Copyright 2001, AIP Publishing.

potential candidate for the applications in microphotonic crystal devices and chips. Early template methods may include complicated and very time-consuming lithography processes, such as[87,93] a 2D hydrophilic- or hydrophobic-templated substrate such as a silane-modified TiO_2 film patterned with ultraviolet (UV) irradiation.[94] By repeating the process, composite PCS patterns can be obtained further to create 3D colloidal crystals by this 2D-patterned substrate. The structures produced in this method have a higher order than those by some chemical template methods. Inkjet printing by Song et al. later can achieve a more precise control of the colored patterns.[95] During the solvent evaporation process, the three-phase contact line of a single droplet containing colloidal particles tends to pin on the hydrophilic points and asymmetrically dewets the hydrophobic region, which results in lines, quadrilaterals, stars, hexagons, octagons, and so on. The strategy of the patterned substrate inducing colloidal PCS patterning can build highly ordered structures; therefore, it can show brighter structural colors, as shown in **Figure 12**. Compared with the 2D-patterned substrate, a droplet containing several monodispersed colloidal particles could be a 3D template for forming spherical PCSs after the evaporation of the solvent.

Due to the weak interaction between colloidal particles, the microspheres assembled by packing are not stable enough to support their uses for practical applications. Much effort has been made by researchers to overcome the disadvantages of those PCSs. First is to induce high-temperature sintering after assembly.[96–98] The bonding between the colloidal particles can be enhanced and the mechanical properties will be improved by high temperature. As shown in **Figure 13**, the surface of the microspheres obtained by this method was smooth and the colloidal particles inside the sphere were arranged in a standard hexagonal-packed structure.[97] Second, a hydrogel monomer can be induced into the dispersion medium to lock the cross-linked network-like solid hydrogel through photopolymerization.[99] As shown in **Figure 14**, the locked SiO_2 colloidal particles into an elastomer can effectively form a nonclose-packed PCS (NCPP) array.[100] By this way, the problem of low elastic

modulus in NCPP colloidal particles will be settled as it has been proven that NCPPs possess better optical properties than their close-packed counterparts.[101]

3.2. Amorphous Colloidal Arrays

In contrast to PCSs, photonic amorphous structures (PASs) are more common in many living organisms in nature, such as blue tarantula hairs with rotational symmetry and hierarchy multilayer structures, blue bird feathers with an amorphous submicron-sized fine air cavities array, genus Morpho butterflies with multilayered disorder ridges, and so on.[102–104] With only short-range order and composed of monodisperse colloidal nanospheres, PASs are also the most commonly designed artificial nanostructures due to their excellent optical properties. As shown in Figure 10b, the lack of long-range order in PASs can avoid the interferences of light and enhance the scattering effect. At the same time, Miyazaki and co-workers have raised a hypothesis that PASs can as well form a similar PBG like PCSs, which is caused by the coherent interference of scattered waves from the periodic structure and the Mie resonances of bonding/antibonding states within each particle.[105] When the scattering effect is not dominant, the main scattering peak (λ_{max}) of PASs (0 order) could be estimated using Bragg–Snell's law

$$\lambda_{max} = 2d(n_{eff}^2 - \sin^2 \alpha)^{1/2} \tag{2}$$

where d is the interplanar spacing of (1 1 1) planes, n_{eff} is the effective refractive index, and α is the incidental angle. Hence, the PASs provide a low-angle-dependent structural color, which would benefit the applications in displays and sensors free from the influence of viewing angles.[106–109] Unlike PCSs, the fabrication of PASs needs more delicate control of the colloidal arrays to present a disordered state. As charged NPs tend to crystallize when the concentration increases,[110,111] many approaches to avoid crystallization have been explored using cohesive particles,[112] bidisperse suspensions,[113,114] or fast drying in the presence of salts.[115]
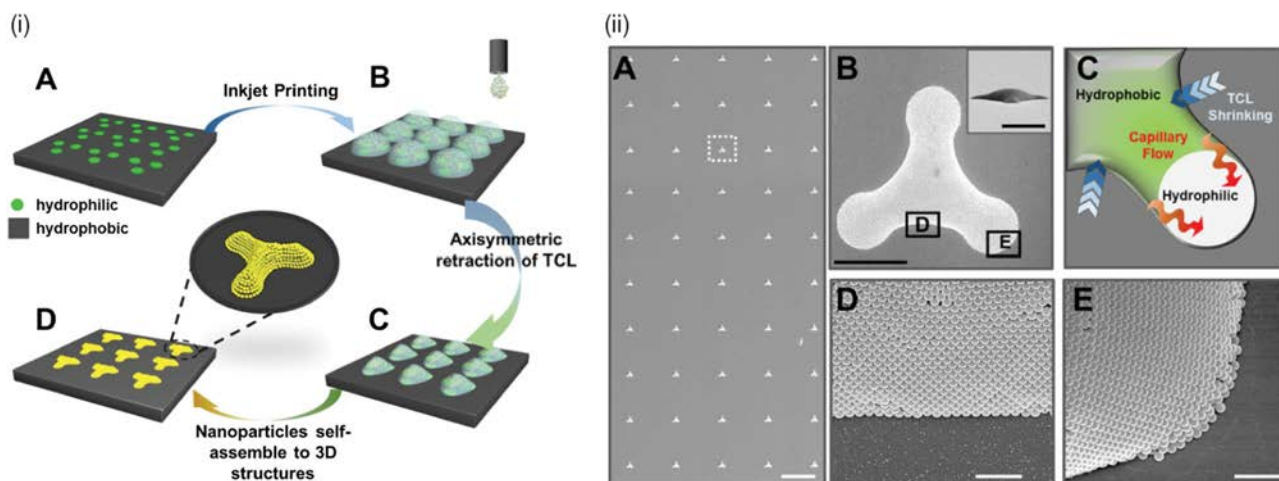

Figure 12. (i) Manipulating 3D morphology of microcolloidal crystal pattern through hydrophilic pattern-induced asymmetric dewetting. (ii) Typical morphology of the 3D microcolloidal crystals induced by hydrophilic pinning pattern. Reproduced with permission.[95] Copyright 2015, WILEY-VCH Verlag GmbH & Co. KGaA, Weinheim.
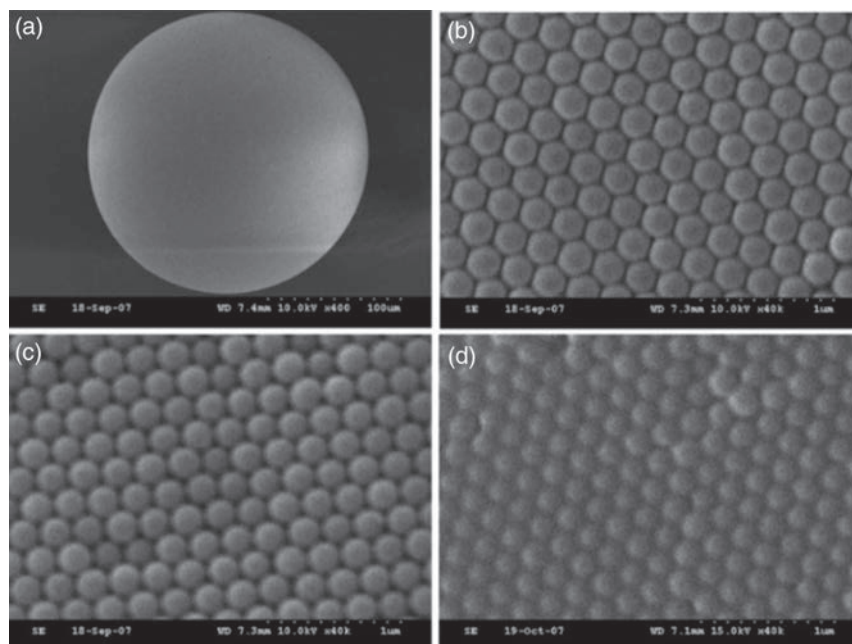
**ADVANCED
SCIENCE NEWS**
www.advancedsciencenews.com

**ADVANCED
INTELLIGENT
SYSTEMS**
Open Access
www.advintellsyst.com

Figure 13. SEM images of CCBs: a) low-magnification image of a bead with a diameter of 200 μm; b,c) bead surface before and after calcination at 700 °C; and d) bead surface after calcination at 1100 °C. Reproduced with permission.[97] Copyright 2008, American Chemical Society.
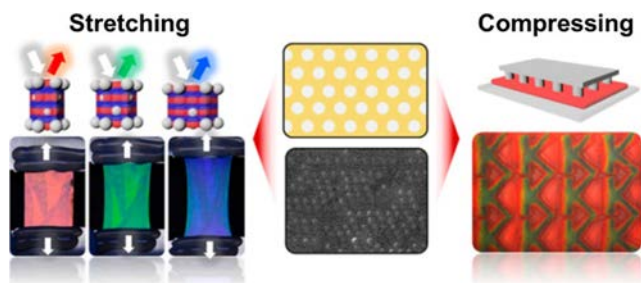

Figure 14. Photonic films containing a nonclose-packed fcc array of SiPs embedded in an elastomer, in which inelastic particles enable elastic deformation and reversible color change, as chameleons do. Reproduced with permission.[100] Copyright 2017, American Chemical Society.

Takeoka and co-workers first prepared the thermoresponsive fine cohesive core–shell particles, in which the core is a monodisperse silica particle (SiP) and the shell is a high-density polymer brush of uniform thickness made from thermally responsive poly(*N*-isopropylacrylamide) (PNIPA).[112] The detailed synthesis of these particles is shown in **Figure 15**. By using a centrifugation technique, the resulting particles could be isolated from the solution, including the free polymers and unreacted monomer. Because the particles randomly adhere to each other, such particles would not crystallize and prefer to form an amorphous array in water. Once the aggregates composed of the amorphous arrays form, the macroscopic shape can be maintained stable. Moreover, the aggregates reveal the responsiveness to the changes occurring in water as a result of temperature variations.

Previous amorphous colloidal arrays have been mostly prepared by mixing two different kinds of submicrometer-sized SiPs, but the colors are too pale to be applicable.[114,116,117]

Yoshioka and co-workers later report a simple and reproducible synthetic procedure for the preparation of amorphous colloidal arrays that exhibit angle-independent, bright structural colors by spraying fine submicrometer-sized spherical SiPs of uniform size.[113] By adding black particles like carbon black (CB) to the colloidal amorphous array, the saturation of the structural color can be enhanced by reducing incoherent light scattering across the entire visible spectrum. The suspension is air sprayed onto a glass plate positioned from the outlet of the spraying nozzle. Because the solvent evaporated rapidly, the SiPs are dried in air and then coated in a powdery state on the glass plate to form a membrane. During the process, rapid evaporation and the choice of appropriate solvent is necessary to obtain an amorphous state of the colloidal particles. **Figure 16** shows the comparisons in the membranes prepared with different weight ratios of CB.

4. Applications

After investigating carefully the fabrication process of structural color materials in the last section, it can be inferred that the stimuli-responsive characteristic in the materials can be used in many intelligent systems, especially for sensors, displays, anticounterfeiting, smart devices, and so on.[9,118] Inspired by the fast and invertible color-shifting phenomena in natural biosystems, three main strategies have been considered for adjusting the optical signals to determine the transmission and reflection of visible light: changes in the refractive indices, tilting the glancing angle, and manipulating the photonic nanostructures. With the implantation of active stimuli-responsive modalities, such as building blocks, matrix, or filtrating ingredients,[119–121] external triggers including temperature, light, ionic or molecular concentration,
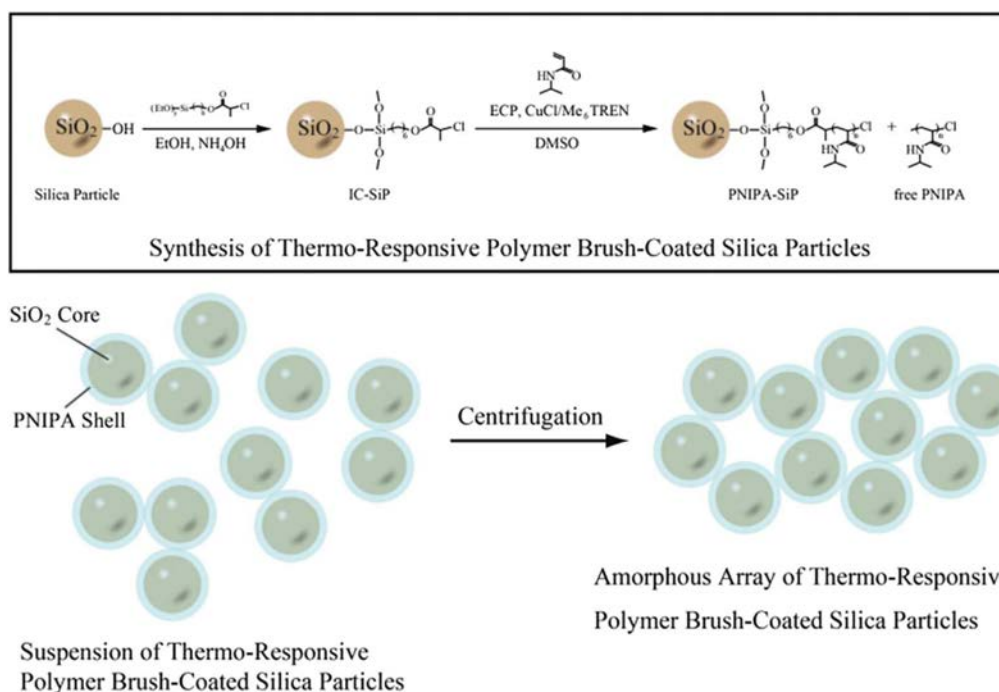
**ADVANCED
SCIENCE NEWS**
www.advancedsciencenews.com

**ADVANCED
INTELLIGENT
SYSTEMS**
www.advintellsyst.com

Figure 15. Schematic procedure for the synthesis of thermoresponsive polymer brush-coated SiPs and the formation of an amorphous array of thermoresponsive polymer brush-coated SiPs. Reproduced with permission.[112] Copyright 2012, Royal Society of Chemistry.
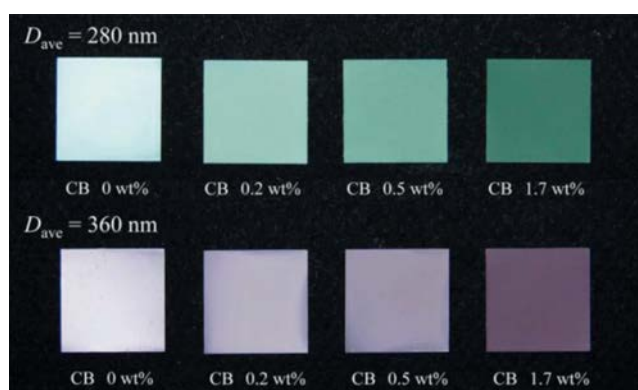

Figure 16. Optical photographs showing the color change in particle membranes with varying quantities of CB. Reproduced with permission.[113] Copyright 2013, WILEY-VCH Verlag GmbH & Co. KGaA, Weinheim.

electric or magnetic field, and mechanical strain can induce the variations among the refractive indices, glancing angle, and photonic nanostructures.[122–127]

4.1. Microfluidic Chip System

Microfluidics has attracted notable interest in growing fields of chemical and biological applications.[128,129] The microfluidic system facilitates many integrated functions for practical utilizations, including mixing, separation, optic-/electric-/thermofunctions, detection, and so on. Using novel functional materials to increase the functions and feasibility of the microfluidic devices is in

greater demand. Incorporation of photonic crystal (PC) materials is one of the attractive candidates that can increase the potential capabilities of optics/photonics and microfluidics,[130–132] due to their characteristics of periodic variation of the dielectric permittivity at wavelength scale and the photonic stop band which is sensitive to the environmental refractive index. Moreover, new functions will be induced into the microfluidic chips by superior properties of PC. The PC can play a role as not only an indicator of the fluid moving in the channel but also an on-chip label-free colorimetric sensor to specific analytes.[133] In addition, the PC is adaptable and tunable to the microfluidic system,[83,134] which can introduce novel applications into the microfluidic devices, such as the localized optical manipulation and response in channels. Gu and co-workers have reported a pseudopaper microfluidic chip based on patterned photonic nitrocellulose with the PCS channels fabricated by sacrificing opal SiO_2 NP templates as shown in **Figure 17**.[135] Because of its capillarity and hydrophilicity, the flow profile of the aqueous solution wicking through the channel is more uniform than for a conventional paper having randomly distributed cellulose microfibers so that it can improve the reproducibility of reagent redissolution and mixing. Also, by altering the size of the NPs which determined the pore size of the PCS channel, the wicking rate of the aqueous solution through the hollow channel could be controlled easily. In this way, the PBG of PCSs can also control the propagation of light, enhance spontaneous radiation, and provide a new way to enhance the sensitivity of fluorescence detection. Later then, by adding the fluorescence enhancement effects of structural color, Gu and co-workers have discovered a new way for the detection of adenosine triphosphate (ATP) and thrombin for the fabrication of analytical capillary devices for
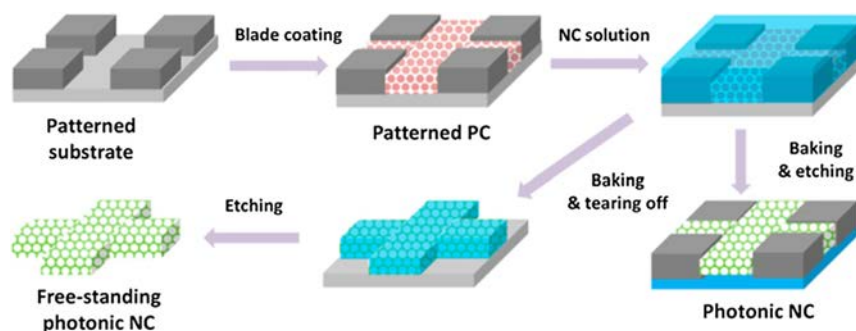
**ADVANCED
SCIENCE NEWS**

www.advancedsciencenews.com

**ADVANCED
INTELLIGENT
SYSTEMS**
Open Access

www.advintellsyst.com

Figure 17. Schematic illustration showing the procedure for fabrication of the patterned photonic nitrocellulose (NC). Reproduced with permission.[135] Copyright 2016, American Chemical Society.

real-time testing with details as described in **Figure 18**a.[136] Attributed to the fluorescence enhancement effect of the photonic heterostructures, the fluorescent signal for detection could be amplified by a factor of up to 40. To achieve more convenience in real-life applications, a wearable monitoring sensor as shown in Figure 18b detecting two proteins (i.e., IgG and AD7c-NTP) based on this fluorescence enhancement effect of structural color has been fabricated, remarkably with high sensitivity detection.[137] The wearable sensor is designed by combining the flexible electronic sensor and microfluidic analytical device as well as placing on a Morpho menelaus. This can be a huge boost for the easy diagnosis of neurodegenerative disease.[136] Moreover, as shown in Figure 18c, further studies through integrating the photonic colloidal crystal in the paper channels have as well been developed with a fish-like biosensor to realize the sweat collection, diagnostics, and fluorescence enhancement detection for sweat lactic acid and urea.[138]

4.2. Optical Display

In addition, a huge demand for advanced display technology is placed with the rapid development of mobile and electronic devices and becoming increasingly important in our daily life. Owing to the low power consumption as well as full-color emission, structural color materials are highly hopeful for constructing optical display devices.[139–141] In particular, the production of a tunable pattern with well-arranged primary colors of red, green, and blue (RGB) units is anticipated, which can be achieved via colloidal assembly along with other techniques like micromolding, printing, or lithography. For example, Kim and co-workers have created a multicolored inverse opal micropattern via combining colloidal self-assembly with the photolithography technique for the further application in reflection-mode display, as shown in **Figure 19**.[142] By the evaporation-induced convective assembly, colloidal crystals are vertically deposited onto the surface of a photoresist. Subsequently, the crystals would then be fully embedded in a photoresist matrix by capillary wetting during thermal annealing. After the next step of photolithography in the photoresist, composite micropatterned structures are formed. This photoresist-based photolithography provides a high definition and flexibility on the patterned shape. The following selective removal of the colloids leaves regular cavities and results in inverse opal structures with high index contrast between the

air and the polymerized photoresist. Thus, the finally created structure provides high reflectivity at the wavelength of the bandgap. With this flexible approach, they also pixelate inverse opals with three distinctive squares of red (R), green (G), and blue (B) structural colors with different cavity sizes, respectively. This kind of pixelated color pattern provides a precondition for implementation of color display devices operated at reflection mode. Furthermore, the switchable function can be affixed via the incorporation of magnetic NPs in alignment with the magnetic field.[139,143] Because of the effect of Bragg's diffraction, most PCS materials show different structural colors when observed from different angles, resulting in brilliant colors and important applications.[144] Enlightened by this, Gu and co-workers make novel PCS with the desired feature of either anisotropic angle independence or full angle independence using colloidal crystal fibers (CCFs) or colloidal crystal beads (CCBs) as their elements with the details given in **Figure 20**. Together with cylinders composed of colloidal crystal arrays, CCFs can show identical reflective color around the center axis and angle-dependent colors along the axis. Also, CCBs demonstrate the spherical symmetry of identical photonic responses independent of the rotation of the axes. Hence, when viewed at different angles, PCS derived from the replication of CCB arrays can display identical structural colors. The prepared PCS film materials are further revealed to be used as photonic papers with vivid colors, wide viewing angles, and rewritable surfaces. For flexible writing and erasing, the salt solution is introduced as an ink due to the ionic-responsive color change behavior of the hydrogel-based inverse opal structure, as shown in **Figure 21**.

4.3. Sensors

Specific colors of PCS materials are caused by distinct wavelengths of reflection, which is determined from the distance between the layers or spheres. As the periodicity of the crystal can be affected by external stimulus, changes in the wavelength of maximum reflectance would lead to the application for probing any target in a complex environment. Such effect is even amenable to visual readout by unskilled operators. Moreover, features of high specificity, sensitivity, as well as low cost have made them more attractive than other kinds of stimuli-responsive materials.[60] It therefore has no doubt that such color changes
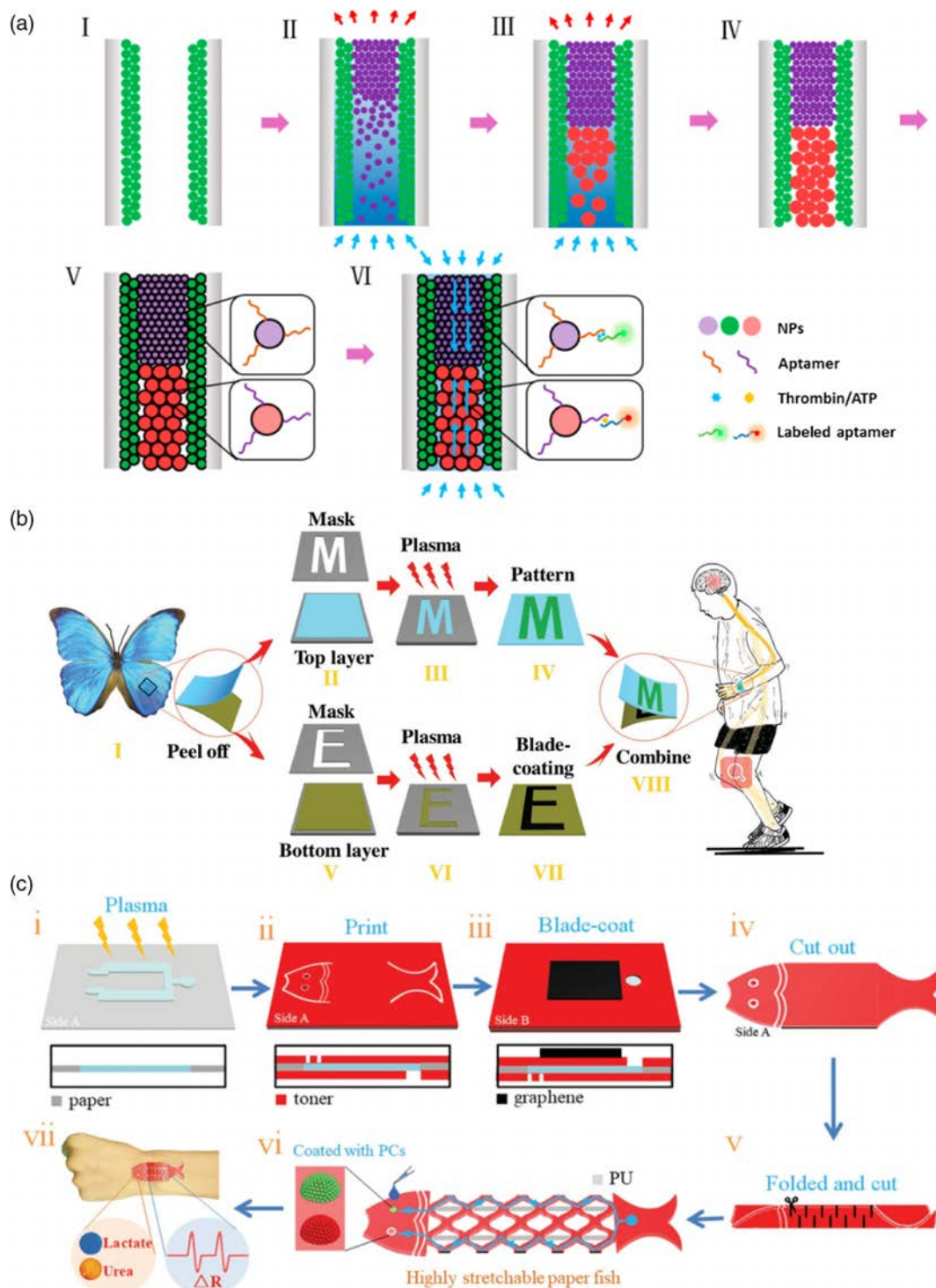
ADVANCED
SCIENCE NEWS

www.advancedsciencenews.com

ADVANCED
INTELLIGENT
SYSTEMS
Open Access

www.advintellsyst.com

Figure 18. Schematic illustration of a) the procedure to fabricate the opal capillary with multiple heterostructures for enhanced fluorescent aptamer-based assays. Reproduced with permission.[136] Copyright 2017, American Chemical Society. b) The fabrication of M. menelaus-based wearable sensors. Reproduced with permission.[137] Copyright 2018, WILEY-VCH Verlag GmbH & Co. KGaA, Weinheim. c) The paper fish sensor fabrication process. Reproduced with permission.[138] Copyright 2018, WILEY-VCH Verlag GmbH & Co. KGaA, Weinheim.

become useful tools for a variety of physical, chemical, and biological sensors.[145–147] For physical sensors, devices made of corresponding PCSs are responsive to physical stimuli, including

mechanical stress (stretching or compression), temperature, external electrical or magnetic field signal, and UV/vis light. Asher et al. described a composite film consisting of PS colloids
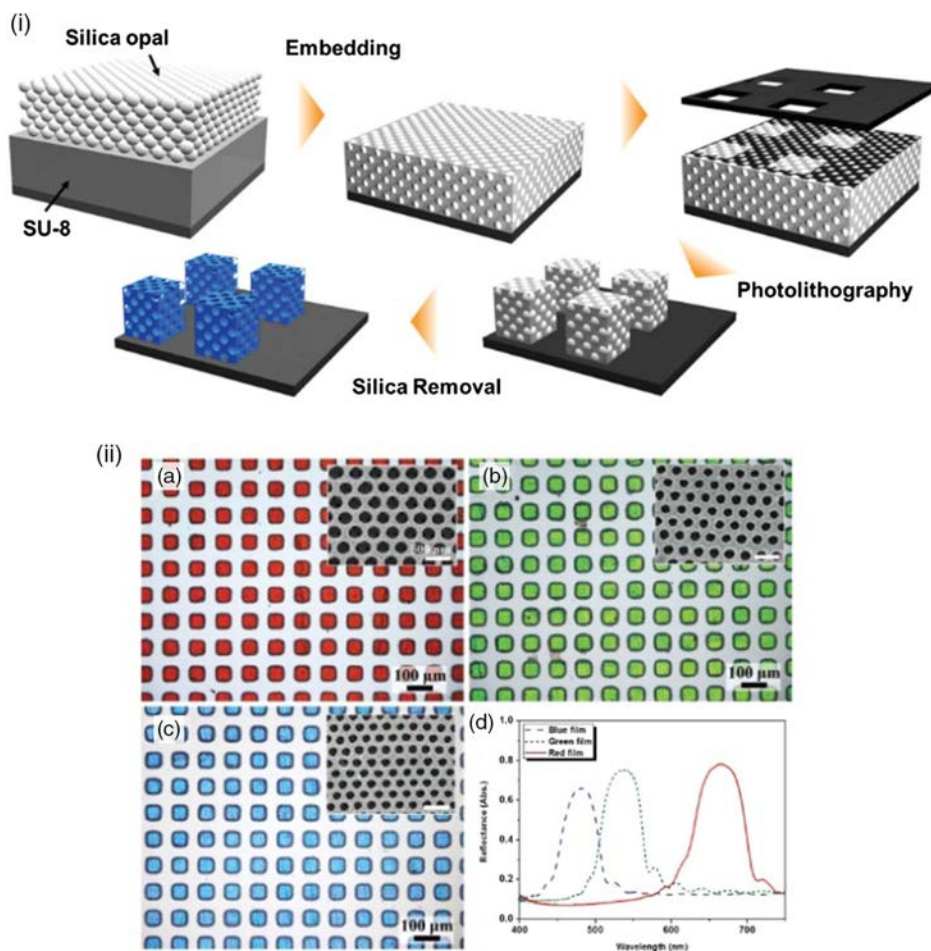
ADVANCED
SCIENCE NEWS
www.advancedsciencenews.com

ADVANCED
INTELLIGENT
SYSTEMS
Open Access
www.advintellsyst.com

Figure 19. (i) Schematic diagram illustrating the formation of a pixelated inverse opal. (ii) (a–c) optical microscope (OM) images of the pixelated inverse opals prepared to reflect a single color. The inverse opals were templated from the opals composed of SiPs of diameter a) 343, b) 278, or c) 249 nm. The insets in each panel show the hexagonal arrays of air cavities on the top surfaces of the pixels. d) The reflectance spectra of the inverse opal films that had been templated by the opals used to prepare (a–c). Reproduced with permission.[142] Copyright 2014, WILEY-VCH Verlag GmbH & Co. KGaA, Weinheim.
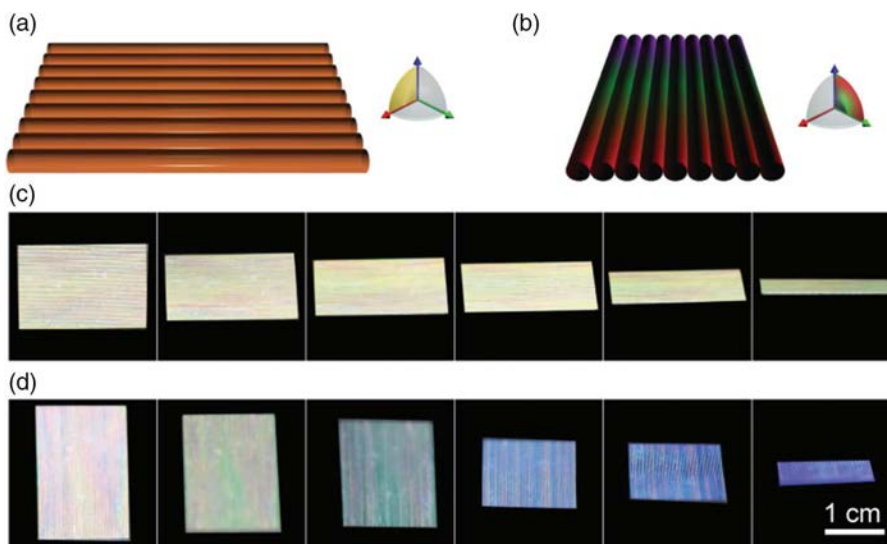

Figure 20. a,b) Schematic diagrams and c,d) photographs of the film composed from colloidal crystal fibers (CCFs) observed at the angles from 90° to approximately 10°. Reproduced with permission.[144] Copyright 2013, WILEY-VCH Verlag GmbH & Co. KGaA, Weinheim.
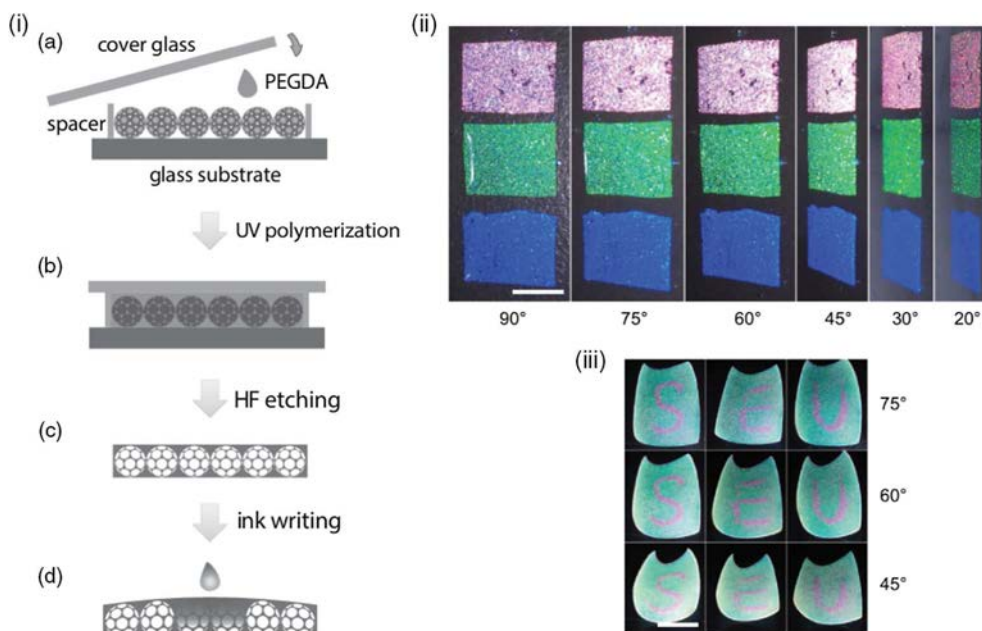
ADVANCED
SCIENCE NEWS

www.advancedsciencenews.com

**ADVANCED
INTELLIGENT
SYSTEMS**
Open Access

www.advintellsyst.com

Figure 21. (i) Schematic illustration of the fabrication and writing test of the photonic paper. (ii) Photographs of three photonic papers viewed at different angles. (iii) A green photonic paper with ink marks of "S", "E", and "U". Reproduced with permission.[144] Copyright 2013, WILEY-VCH Verlag GmbH & Co. KGaA, Weinheim.

embedded in an N-vinylpyrrolidone/acrylamide copolymer. The reflected wavelength maximum shifts from 573 to 538 nm after uniaxial stretching as a result of the reduction in the distance between the particles in the lattice.[78] The process is reversible and recoverable once releasing the pressure. Stability of this kind of polymer can be further improved using other substitute matrix materials. A wavelength shift of 55 nm is observed under a compressive load of 1 kPa and the working pressure range is much wider from 0 to 1000 Pa. However, a better property can be obtained but it would sacrifice its mechanical stability and recovery time.[148,149] Further modification to the polymer has been explored to achieve a water-free, robust, and fast-responding composite tested with a piezoelectric modulator. The total range of the wavelength shift is expanded to 172 nm and is sensitive to modulation frequencies up to 200 Hz, making this material more useful.[150] Thermally responsive PCSs are generally divided into two types: ones based on polymer swelling and others based on phase transitions when incorporated into inorganic host materials. One typical example is from Asher and co-workers' results by combining polymer and PCS materials which are embedded in a thermosensitive hydrogel, such as poly(N-isopropylacrylamide) (PNIPAM).[79] Water in the materials would be removed by PNIPAM from the voids in the polymer when reaching a certain temperature and lead to polymer shrinkage. With reversible change in volume, the corresponding reflected wavelength can cover the entire visible range. The other types of thermally PCS sensors based on phase transitions in inorganic material hosts possess better thermal stability and faster response time than the first type in recent research.[151] By coating with Malachite green carbinol base, surface charge of silica nanospheres can be altered upon UV irradiation. In this case, changes in the lattice distance by phase transition would cause the refractive

index change in the PCS and the corresponding wavelength shift. That is a typical example reported for optical sensors.[152]

For chemical sensor systems, they need PCSs responding to chemical stimuli, such as solvents, vapors, and chemical species. Inverse opal is the most common material utilized in this area with a 3D periodic hole structure, such as oxides of silicon, due to the significant changes in refractive index upon solvent altering.[81,153–155] Mesoporous (1D) Bragg stacks consisting of various inorganic materials can differentiate organic solvents particularly well.[156,157]

On the other hand, biosensors containing biological components, such as enzymes, antibodies, aptamers, and gene probes, can detect a specific signal. Such sensors can be applied in the areas of compound libraries and ligand–receptor interactions screening, in label-free optical detection, and cell morphology.[13] For a clinically relevant parameter like creatinine, it can be detected with PCS sensors using the creatinine deiminase enzyme. This can be elucidated by the swelling of hydrogels from two continuous reactions: first is the production of hydroxide ions by hydrolysis of creatinine by creatinine deiminase and second is the deprotonation of 2-nitrophenol (also incorporated in the hydrogel) by the formation of hydroxy ions. The red shift in the diffraction is approximately 35 nm at 1 mm levels of creatinine, of which the sensitivity is much smaller (15 nm) at typical physiological concentrations (100 mm).[158]

4.4. Soft Robotics

Distinctive from conventionally hard-body robotics made of rigid materials to perform one single task efficiently with limited adaptability, soft robots can erase the obstacle between machines

**ADVANCED
SCIENCE NEWS**
www.advancedsciencenews.com

**ADVANCED
INTELLIGENT
SYSTEMS**
Open Access
www.advintellsyst.com

and people as well as achieve more advanced functions like movement, perception, communication, and so on. Due to the similarity to natural systems, these robots with a continuously transmutable structure are of much higher order of freedom than their hard-bodied counterparts.[159] Therefore, new classes of functional materials have to be explored to realize and perfect this application. Structural color materials are mainly developed in the actuation systems in a robot. Triggered by external stimuli, Zhang and co-workers incorporate PCs with deformable materials for bending actuation through humidity responsiveness.[160] Another thermal-triggered PC actuator has been discovered by Wei et al. using an inverse opal/liquid crystal elastomer (LCE) bilayer film.[161] It has been demonstrated that the asymmetric shrinkage/expansion behavior of the bilayer is driven by temperature changes and finally results in a bending deformation and color change of the film. In addition, Chen and co-workers report a light-triggered actuator by means of a laminated film combination of a polydimethylsiloxane (PDMS)-infiltrated colloidal crystal layer and a single-walled carbon nanotube (SWCN)–LCE layer separated by a PDMS glue.[162] The film could perform the corresponding

localized actuation upon infrared (IR) irradiation. Furthermore, to complete more complex and selective actuation, Guo and co-workers further develop a structural colored bionic hand by coupling inverse opal and graphene oxide (GO) as a thermal–mechanical unit and photothermal conversion component.[163]

All-round actuation modes and the corresponding deformation behaviors result in real hand mimic actions, as shown in **Figure 22**. Unlike methods relying on external triggers, a self-actuated mode can also be obtained, such as a 3D artificial Morpho butterfly.[10] By using a structural color hydrogel with radial microgroove patterns, cardiomyocytes are in a laminar assembly. This way, the swinging of butterfly wings would be caused upon the anisotropic cell contraction and relaxation.

5. Conclusions and Outlook

A combination of the bottom-up colloidal self-assembly and the top-down lithography techniques has achieved great success for the fabrication of periodic structural color materials due to the advantages of versatility and scalability. Several main methods of colloidal assembly, including evaporation, interface, template, and external physical and chemical stimuli, are introduced in this review, helping elucidate the basic rules of how colloidal particles turn into complicated and diverse crystalline and amorphous structures. To improve the uniformity and mechanical stability of the final nanostructures, creative ideas have been put forward, such as importing droplet suspension on hydrophobic surfaces, whereas deeper studies have been investigated on how various parameters like temperature and flow rate affect the structure formation. Based on the outstanding technique, fabrication of
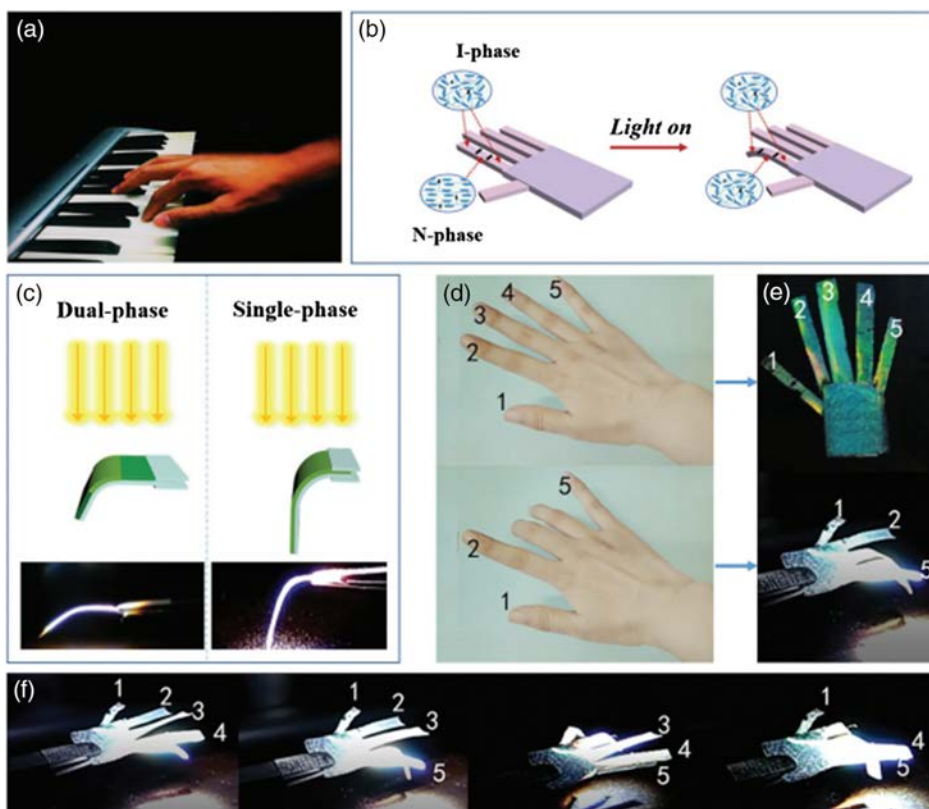

Figure 22. a) Real photo of the action of fingers playing the piano. b) Schematic diagram of the bionic hand based on the LC photonic films. c) Comparison of the bending deformation between the dual-phase film and the single-phase film. d) Finger action of the hand in the real world. e) The corresponding action of bionic hand based on the LC photonic films. f) Series of movement of the bionic hand upon visible light irradiation. Reproduced with permission.[163] Copyright 2018, WILEY-VCH Verlag GmbH & Co. KGaA, Weinheim.

structural color materials has become easier for researchers to explore. Explicitly, two main types of structural color materials are explained in detail according to different principles of interactions with light. Especially for construction of such materials, more functional elements like hydrogel and stimuli groups may be added during the preparation process for further enhanced applications in optical and electrical devices. To conclude, from materials to devices, there is still a long way to go to achieve more complex and smart functions of structural color materials. Although recent progress has been accomplished, challenges still remain as well as huge space for development. First, more thorough studies on natural structural coloration are needed to understand the intriguing color production and perception processes, which are closely associated with multiple-level biological life activities such as behavioral ecology and evolution. This will provide more substantial implications of coloration-related biological functions instead of only the visual appearance. In addition, bio-inspired artificial structural color materials with more complexity require more advanced fabrication techniques and strategies by the help of additive manufacturing or even genetic engineering. In addition, to even suppress nature, other novel synthetic structural color materials can be obtained to achieve more functions by incorporating novel materials, including plasmonic or metal NPs combining optical effects or other features, which are not available in nature. In any case, there is still a pathway for improvement for the advanced intelligent applications. The next-generation devices can be even more intelligent to accommodate more complicated environmental changes and accomplish more customized integration tasks. Finally, to step out of the laboratory stage, the problems of short durability, less portability, robustness, and scalability of structural color materials have to be addressed urgently. The multidiscipline integration of mathematics, structural mechanics, surface chemistry, and so on, may help to build future advanced structural color platforms or devices.

Conflict of Interest

The authors declare no conflict of interest.

[1] R. B. Fletcher, J. Hattie, *Intelligence and Intelligence Testing*, Routledge, London **2011**.

[2] X. Zhang, L. Chen, K. H. Lim, S. Gonuguntla, K. W. Lim, D. Pranantyo, W. P. Yong, W. J. T. Yam, Z. Low, W. J. Teo, H. P. Nien, Q. W. Loh, S. Soh, *Adv. Mater.* **2019**, *31*, 1.

[3] J. Hwang, M. Pototschnig, R. Lettow, G. Zumofen, A. Renn, S. Götzinger, V. Sandoghdar, *Conf. Proc. Lasers Electro-Optics Society Annual Meetings*, IEEE, Piscataway, NJ **2009**, *460*, 286.

[4] I. Ferain, C. A. Colinge, J. P. Colinge, *Nature* **2011**, *479*, 310.

[5] L. Shang, W. Zhang, K. Xu, Y. Zhao, *Mater. Horizons* **2019**, 945.

[6] D. Zhao, R. Wang, *Chem. Soc. Rev.* **2012**, *41*, 2095.

[7] I. C. Cuthill, W. L. Allen, K. Arbuckle, B. Caspers, G. Chaplin, M. E. Hauber, G. E. Hill, N. G. Jablonski, C. D. Jiggins, A. Kelber, J. Mappes, J. Marshall, R. Merrill, D. Osorio, R. Prum, N. W. Roberts, A. Roulin, H. M. Rowland, T. N. Sherratt, J. Skelhorn, M. P. Speed, M. Stevens, M. C. Stoddard, D. Stuart-Fox, L. Talas, E. Tibbetts, T. Caro, *Science* **2017**, *357*, 1.

[8] P. Andrew Richard, *J. Opt. A Pure Appl. Opt.* **2000**, *2*, R15.

[9] J. Ge, Y. Yin, *Angew. Chem. Int. Ed.* **2011**, *50*, 1492.

[10] F. Fu, L. Shang, Z. Chen, Y. Yu, Y. Zhao, *Sci. Robot.* **2018**, *3*, eaar8580.

[11] F. Fu, Z. Chen, Z. Zhao, H. Wang, L. Shang, Z. Gu, Y. Zhao, *Proc. Natl. Acad. Sci. USA* **2017**, *114*, 5900.

[12] N. Vogel, S. Utech, G. T. England, T. Shirman, K. R. Phillips, N. Koay, I. B. Burgess, M. Kolle, D. A. Weitz, J. Aizenberg, *Proc. Natl. Acad. Sci. USA* **2015**, *112*, 10845.

[13] Y. Zhao, X. Zhao, Z. Gu, *Adv. Funct. Mater.* **2010**, *20*, 2970.

[14] A. Thiaville, J. Miltat, *Science* **1999**, *284*, 1939.

[15] G. Konstantatos, E. H. Sargent, *Nat. Nanotechnol.* **2010**, *5*, 391.

[16] Z. Xu, L. Wang, F. Fang, Y. Fu, Z. Yin, *Curr. Nanosci.* **2016**, *12*, 725.

[17] R. Li, X. Yang, G. Li, S. Li, W. Huang, *Langmuir* **2006**, *22*, 8127.

[18] R. H. Ottewill, A. B. Schofield, J. A. Waters, N. St. J. Williams, *Colloid Polym. Sci.* **1997**, *275*, 274.

[19] T. C. Merkel, V. I. Bondar, K. Nagai, B. D. Freeman, I. Pinnau, *J. Polym. Sci. B Polym. Phys.* **2000**, *38*, 415.

[20] G. Li, X. Yang, F. Bai, W. Huang, *J. Colloid Interface Sci.* **2006**, *297*, 705.

[21] X. Ye, L. Qi, *Nano Today* **2011**, *6*, 608.

[22] J. Zhang, Y. Li, X. Zhang, B. Yang, *Adv. Mater.* **2010**, *22*, 4249.

[23] J. Tian, J. Jin, F. Zheng, H. Zhao, *Langmuir* **2010**, *26*, 8762.

[24] N. D. Denkov, O. D. Velev, P. A. Kralchevsky, I. B. Ivanov, *Langmuir* **1992**, *8*, 3183.

[25] A. Dimitrov, K. Nagayama, *Langmuir* **1996**, *12*, 1303.

[26] S. Choi, A. Jamshidi, T. J. Seok, M. C. Wu, T. I. Zohdi, A. P. Pisano, *Langmuir* **2012**, *28*, 3102.

[27] E. Sowade, T. Blaudeck, R. R. Baumann, *Nanoscale Res. Lett.* **2015**, *10*, 0.

[28] X. Liang, R. Dong, J. C. Ho, *Adv. Mater. Technol.* **2019**, *4*, 1.

[29] R. van Dommelen, P. Fanzio, L. Sasso, *Adv. Colloid Interface Sci.* **2018**, *251*, 97.

[30] W. D. Ruan, Z. C. Lü, N. Ji, C. X. Wang, B. Zhao, J. H. Zhang, *Chem. Res. Chinese Univ.* **2007**, *3*, 712.

[31] L. Isa, K. Kumar, M. Müller, J. Grolig, M. Textor, E. Reimhult, *ACS Nano* **2010**, *4*, 5665.

[32] Y. Lin, A. Böker, H. Skaff, D. Cookson, A. D. Dinsmore, T. Emrick, T. P. Russell, *Langmuir* **2005**, *21*, 191.

[33] A. Böker, J. He, T. Emrick, T. P. Russell, *Soft Matter* **2007**, *3*, 1231.

[34] Z. Nie, A. Petukhova, E. Kumacheva, *Nat. Nanotechnol.* **2010**, *5*, 15.

[35] S. K. Dey, J. F. Stoddart, R. Klajn, K. P. Browne, A. Coskun, L. Fang, M. A. Olson, B. A. Grzybowski, *Nano Lett.* **2009**, *9*, 3185.

[36] M. A. Correa-Duarte, L. M. Liz-Marzán, *J. Mater. Chem.* **2006**, *16*, 22.

[37] Y. Zhao, K. Thorkelsson, A. J. Mastroianni, T. Schilling, J. M. Luther, B. J. Rancatore, K. Matsunaga, H. Jinnai, Y. Wu, D. Poulsen, J. M. J. Fréchet, A. Paul Alivisatos, T. Xu, *Nat. Mater.* **2009**, *8*, 979.

[38] D. Xia, D. Li, Z. Ku, Y. Luo, S. R. J. Brueck, *Langmuir* **2007**, *23*, 5377.

[39] B. Varghese, F. C. Cheong, S. Sindhu, T. Yu, C. T. Lim, S. Valiyaveettil, C. H. Sow, *Langmuir* **2006**, *22*, 8248.

[40] Q. Dai, J. Frommer, D. Berman, K. Virwani, B. Davis, J. Y. Cheng, A. Nelson, *Langmuir* **2013**, *29*, 7472.

[41] L. Malaquin, T. Kraus, H. Schmid, E. Delamarche, H. Wolf, *Langmuir* **2007**, *23*, 11513.

[42] J. Kim, G. S. Hwang, D.-E. Lee, J. Ahn, C.-S. Hwang, B. D. Chin, D. H. Lee, *ACS Appl. Electron. Mater.* **2019**, *1*, 8.

[43] V. Gupta, P. T. Probst, F. R. Goßler, A. M. Steiner, J. Schubert, Y. Brasse, T. A. F. König, A. Fery, *ACS Appl. Mater. Interfaces* **2019**, *11*, 28189.

[44] X. Hu, Z. Xu, K. Li, F. Fang, L. Wang, *Appl. Surf. Sci.* **2015**, *355*, 1168.

[45] Y. Lu, Y. Yin, Y. Xia, *Adv. Mater.* **2001**, 34.

[46] Y. Yin, Y. Lu, Y. Xia, *J. Am. Chem. Soc.* **2001**, *123*, 771.

[47] Y. Yin, Y. Xia, *Adv. Mater.* **2001**, 267.

[48] Y. Yin, Y. Lu, Y. Xia, *J. Mater. Chem.* **2001**, *11*, 987.

[49] Y. Yin, Y. Lu, B. Gates, Y. Xia, R. V April, *J. Am. Chem. Soc.* **2001**, *25*, 8718.

[50] A. P. Gast, C. F. Zukoski, *Adv. Colloid Interface Sci.* **1989**, *30*, 153.

[51] J. D. Jackson, R. F. Fox, *Am. J. Phys.* **1999**, *67*, 841.

[52] R. W. O'Brien, L. R. White, S. C. Particle, *J. Chem. Soc. Faraday Trans.* **1978**, *74*, 1607.

[53] S. Fraden, A. Blaaderen, *J. Chem. Phys.* **2000**, *112*, 3851.

[54] A. P. Hynninen, M. Dijkstra, *Phys. Rev. Lett.* **2005**, *94*, 8.

[55] S. Fraden, R. B. Meyer, *Nature* **2006**, *207*, 1238.

[56] W. T. Thomas, C. Halsey, *Phys. Rev. Lett.* **1990**, *65*, 2820.

[57] Z. M. Sherman, D. Ghosh, J. W. Swan, *Langmuir* **2018**, *34*, 7117.

[58] T. Colla, P. S. Mohanty, S. Nöjd, E. Bialik, A. Riede, P. Schurtenberger, C. N. Likos, *ACS Nano* **2018**, *12*, 4321.

[59] S. O. Lumsdon, E. W. Kaler, O. D. Velev, *Langmuir* **2004**, *20*, 2108.

[60] M. A. C. Stuart, W. T. S. Huck, J. Genzer, M. Müller, C. Ober, M. Stamm, G. B. Sukhorukov, I. Szleifer, V. V. Tsukruk, M. Urban, F. Winnik, S. Zauscher, I. Luzinov, S. Minko, *Nat. Mater.* **2010**, *9*, 101.

[61] A. B. Descalzo, R. Martínez-Máñez, F. Sancenón, K. Hoffmann, K. Rurack, *Angew. Chem. Int. Ed.* **2006**, *45*, 5924.

[62] M. Grzelczak, L. M. Liz-Marzán, R. Klajn, *Chem. Soc. Rev.* **2019**, *48*, 1342.

[63] W. Lv, C. Zhang, Z. Li, Q. H. Yang, *J. Phys. Chem. Lett.* **2015**, *6*, 658.

[64] Y. Xu, G. Shi, *J. Mater. Chem.* **2011**, *21*, 3311.

[65] H. Zhang, D. Wang, *Angew. Chem. Int. Ed.* **2008**, *47*, 3984.

[66] Z. Yin, W. Zhang, Q. Fu, H. Yue, W. Wei, P. Tang, W. Li, W. Li, L. Lin, G. Ma, D. Ma, *Small* **2014**, *10*, 3619.

[67] A. R. Parker, *J. Opt. A Pure Appl. Opt.* **2000**, *2*, 15.

[68] S. Tadepalli, J. M. Slocik, M. K. Gupta, R. R. Naik, S. Singamaneni, *Chem. Rev.* **2017**, *117*, 12705.

[69] Y. Zhao, Z. Xie, H. Gu, C. Zhu, Z. Gu, *Chem. Soc. Rev.* **2012**, *41*, 3297.

[70] S. Kinoshita, S. Yoshioka, J. Miyazaki, *Rep. Prog. Phys.* **2008**, *71*, 076401.

[71] E. S. A. Goerlitzer, R. N. Klupp Taylor, N. Vogel, *Adv. Mater.* **2018**, *30*, 1.

[72] M. Arcari, I. Söllner, A. Javadi, S. Lindskov Hansen, S. Mahmoodian, J. Liu, H. Thyrrestrup, E. H. Lee, J. D. Song, S. Stobbe, P. Lodahl, *Phys. Rev. Lett.* **2014**, *113*, 1.

[73] J. D. Joannopoulos, P. R. Villeneuve, S. H. Fan, *Nature* **1997**, *387*, 830.

[74] J. Hou, M. Li, Y. Song, *Angew. Chem. Int. Ed.* **2018**, *57*, 2544.

[75] Eli Yablonovitch, *Phys. Rev. Lett.* **1987**, *58*, 13.

[76] S. John, *Phys. Rev. Lett.* **1987**, *58*, 2486.

[77] P. Liu, L. Bai, J. Yang, H. Gu, Q. Zhong, Z. Xie, Z. Gu, *Nanoscale Adv.* **2019**, *1*, 1672.

[78] S. A. Asher, J. Holtz, L. Liu, Z. Wu, *J. Am. Chem. Soc.* **1994**, *116*, 4997.

[79] J. M. Weissman, H. B. Sunkara, A. S. Tse, S. A. Asher, *Science* **1996**, *274*, 959.

[80] O. L. Pursiainen, J. J. Baumberg, H. Winkler, B. Viel, P. Spahn, T. Ruhl, *Opt. Express* **2007**, *15*, 9553.

[81] V. N. Bogomolov, S. V Gaponenko, A. M. Kapitonov, E. P. Petrov, N. V Gaponenko, A. V. P. Ev, A. N. Ponyavina, N. I. Silvanovich, S. M. Samoilovich, *Phys. Rev. E* **1997**, *55*, 7619.

[82] R. Mayoral, J. Requena, J. S. Moya, C. Lbpez, A. Cintas, H. Miguez, F. Meseguer, L. Vazquez, M. Holgado, A. Blunco, *Adv. Mater.* **1997**, 257.

[83] G. Widawski, M. Rawiso, B. François, *Nature* **1994**, *369*, 387.

[84] S. H. Park, Y. Xia, *Adv. Mater.* **1998**, *10*, 1045.

[85] P. Jiang, J. F. Bertone, K. S. Hwang, V. L. Colvin, *Chem. Mater.* **1999**, *11*, 2132.

[86] O. S. Q.-B. Meng, Z.-Z. Gu, *Appl. Phys. Lett.* **2000**, *77*, 4313.

[87] S. M. Yang, H. Míguez, G. A. Ozin, *Adv. Funct. Mater.* **2002**, *12*, 425.

[88] Y. A. Vlasov, X. Z. Bo, J. C. Sturm, D. J. Norris, *Nature* **2001**, *414*, 289.

[89] Z. Z. Gu, A. Fujishima, O. Sato, *Chem. Mater.* **2002**, *14*, 760.

[90] Z. Z. Gu, Q. B. Meng, S. Hayami, A. Fujishima, O. Sato, *J. Appl. Phys.* **2001**, *90*, 2042.

[91] J. Chen, P. Dong, D. Di, C. Wang, H. Wang, J. Wang, X. Wu, *Appl. Surf. Sci.* **2013**, *270*, 6.

[92] Z. Z. Gu, D. Wang, H. Möhwald, *Soft Matter* **2007**, *3*, 68.

[93] P. V. Braun, R. W. Zehner, C. A. White, M. K. Weldon, C. Kloc, S. S. Patel, P. Wiltzius, *Adv. Mater.* **2001**, *13*, 721.

[94] Z. Z. Gu, A. Fujishima, O. Sato, *Angew. Chem. Int. Ed.* **2002**, *41*, 2067.

[95] L. Wu, Z. Dong, M. Kuang, Y. Li, F. Li, L. Jiang, Y. Song, *Adv. Funct. Mater.* **2015**, *25*, 2237.

[96] Y. Zhao, X. Zhao, J. Hu, M. Xu, W. Zhao, L. Sun, C. Zhu, H. Xu, Z. Gu, *Adv. Mater.* **2009**, *21*, 569.

[97] Y. Zhao, X. Zhao, C. Sun, J. Li, R. Zhu, Z. Gu, *Anal. Chem.* **2008**, *80*, 1598.

[98] X. Zhao, Y. Cao, F. Ito, H. H. Chen, K. Nagai, Y. H. Zhao, Z. Z. Gu, *Angew. Chem. Int. Ed.* **2006**, *45*, 6835.

[99] Z. Chen, M. Mo, F. Fu, L. Shang, H. Wang, C. Liu, Y. Zhao, *ACS Appl. Mater. Interfaces* **2017**, *9*, 38901.

[100] G. H. Lee, T. M. Choi, B. Kim, S. H. Han, J. M. Lee, S. H. Kim, *ACS Nano* **2017**, *11*, 11350.

[101] F. Meseguer, R. Fenollosa, *J. Mater. Chem.* **2005**, *15*, 4577.

[102] K. Chung, S. Yu, C. J. Heo, J. W. Shim, S. M. Yang, M. G. Han, H. S. Lee, Y. Jin, S. Y. Lee, N. Park, J. H. Shin, *Adv. Mater.* **2012**, *24*, 2375.

[103] Y. Takeoka, *J. Mater. Chem.* **2012**, *22*, 23299.

[104] B. K. Hsiung, R. H. Siddique, L. Jiang, Y. Liu, Y. Lu, M. D. Shawkey, T. A. Blackledge, *Adv. Opt. Mater.* **2017**, *5*, 1.

[105] H. Miyazaki, M. Hase, H. T. Miyazaki, Y. Kurokawa, N. Shinya, *Phys. Rev. B: Condens. Matter Mater. Phys.* **2003**, *67*, 1.

[106] W. Yuan, N. Zhou, L. Shi, K. Q. Zhang, *ACS Appl. Mater. Interfaces* **2015**, *7*, 14064.

[107] Y. Meng, B. Tang, B. Ju, S. Wu, S. Zhang, *ACS Appl. Mater. Interfaces* **2017**, *9*, 3024.

[108] A. C. Arsenault, D. P. Puzzo, I. Manners, G. A. Ozin, *Nat. Photonics* **2007**, *1*, 468.

[109] I. Lee, D. Kim, J. Kal, H. Baek, D. Kwak, D. Go, E. Kim, C. Kang, J. Chung, Y. Jang, S. Ji, J. Joo, Y. Kang, *Adv. Mater.* **2010**, *22*, 4973.

[110] D. J. Norris, E. G. Arlinghaus, L. Meng, R. Heiny, L. E. Scriven, *Adv. Mater.* **2004**, *16*, 1393.

[111] O. D. Velev, *Science* **2000**, *287*, 2240.

[112] Y. Gotoh, H. Suzuki, N. Kumano, T. Seki, K. Katagiri, Y. Takeoka, *New J. Chem.* **2012**, *36*, 2171.

[113] Y. Takeoka, S. Yoshioka, A. Takano, S. Arai, K. Nueangnoraj, H. Nishihara, M. Teshima, Y. Ohtsuka, T. Seki, *Angew. Chem. Int. Ed.* **2013**, *52*, 7261.

[114] J. D. Forster, H. Noh, S. F. Liew, V. Saranathan, C. F. Schreck, L. Yang, J. C. Park, R. O. Prum, S. G. J. Mochrie, C. S. O'Hern, H. Cao, E. R. Dufresne, *Adv. Mater.* **2010**, *22*, 2939.

[115] Y. Takeoka, S. Yoshioka, M. Teshima, A. Takano, M. Harun-Ur-Rashid, T. Seki, *Sci. Rep.* **2013**, *3*, 1.

[116] S. F. Liew, J. Forster, H. Noh, C. F. Schreck, V. Saranathan, X. Lu, L. Yang, R. O. Prum, C. S. O'Hern, E. R. Dufresne, H. Cao, *Opt. Express* **2011**, *19*, 8208.

[117] M. Harun-Ur-Rashid, A. Bin Imran, T. Seki, M. Ishii, H. Nakamura, Y. Takeoka, *ChemPhysChem* **2010**, *11*, 579.

[118] H. Fudouzi, *Sci. Technol. Adv. Mater.* **2011**, *12*, 6.

[119] C. Liu, H. Ding, Z. Wu, B. Gao, F. Fu, L. Shang, Z. Gu, Y. Zhao, *Adv. Funct. Mater.* **2016**, *26*, 7937.

[120] D. Ge, E. Lee, L. Yang, Y. Cho, M. Li, D. S. Gianola, S. Yang, *Adv. Mater.* **2015**, *27*, 2489.

[121] B. F. Ye, Y. J. Zhao, Y. Cheng, T. T. Li, Z. Y. Xie, X. W. Zhao, Z. Z. Gu, *Nanoscale* **2012**, *4*, 5998.

[122] N. Jiang, H. Butt, Y. Montelongo, F. Liu, S. Afewerki, G. L. Ying, Q. Dai, S. H. Yun, A. K. Yetisen, *Adv. Funct. Mater.* **2018**, *28*, 1.

[123] K. Yao, Q. Meng, V. Bulone, Q. Zhou, *Adv. Mater.* **2017**, *29*, 1.

[124] H. K. Bisoyi, Q. Li, *Acc. Chem. Res.* **2014**, *47*, 3184.

[125] J. E. Stumpel, E. R. Gil, A. B. Spoelstra, C. W. M. Bastiaansen, D. J. Broer, A. P. H. J. Schenning, *Adv. Funct. Mater.* **2015**, *25*, 3314.

[126] A. C. Arsenault, T. J. Clark, G. Von Freymann, L. Cademartiri, R. Sapienza, J. Bertolotti, E. Vekris, S. Wong, V. Kitaev, I. Manners, R. Z. Wang, S. John, D. Wiersma, G. A. Ozin, *Nat. Mater.* **2006**, *5*, 179.

[127] M. Wang, Y. Yin, *J. Am. Chem. Soc.* **2016**, *138*, 6315.

[128] M. I. Mohammed, M. P. Y. Desmulliez, *Lab Chip* **2011**, *11*, 569.

[129] J. S. Kuo, D. T. Chiu, *Lab Chip* **2011**, *11*, 2656.

[130] D. Psaltis, S. R. Quake, C. Yang, *Nature* **2006**, *442*, 381.

[131] S. H. Kim, J. W. Shim, S. M. Yang, *Angew. Chem. Int. Ed.* **2011**, *50*, 1171.

[132] D. Erickson, X. Serey, Y. F. Chen, S. Mandal, *Lab Chip* **2011**, *11*, 995.

[133] W. Qian, Z. Z. Gu, A. Fujishima, O. Sato, *Langmuir* **2002**, *18*, 4526.

[134] C. Sun, X. W. Zhao, Y. J. Zhao, R. Zhu, Z. Z. Gu, *Small* **2008**, *4*, 592.

[135] B. Gao, H. Liu, Z. Gu, *Anal. Chem.* **2016**, *88*, 5424.

[136] B. Gao, L. Tang, D. Zhang, Z. Xie, E. Su, H. Liu, Z. Gu, *ACS Appl. Mater. Interfaces* **2017**, *9*, 32577.

[137] Z. He, A. Elbaz, B. Gao, J. Zhang, E. Su, Z. Gu, *Adv. Healthc. Mater.* **2018**, *7*, 1.

[138] B. Gao, A. Elbaz, Z. He, Z. Xie, H. Xu, S. Liu, E. Su, H. Liu, Z. Gu, *Adv. Mater. Technol.* **2018**, *3*, 1.

[139] Z. Yu, C. F. Wang, L. Ling, L. Chen, S. Chen, *Angew. Chem. Int. Ed.* **2012**, *51*, 2375.

[140] H. S. Lee, T. S. Shim, H. Hwang, S. M. Yang, S. H. Kim, *Chem. Mater.* **2013**, *25*, 2684.

[141] Y. Zhao, Y. Zhao, S. Hu, J. Lv, Y. Ying, G. Gervinskas, G. Si, *Materials* **2017**, *10*, 944.

[142] S. Y. Lee, S. H. Kim, H. Hwang, J. Y. Sim, S. M. Yang, *Adv. Mater.* **2014**, *26*, 2391.

[143] Y. Zhao, L. Shang, Y. Cheng, Z. Gu, *Acc. Chem. Res.* **2014**, *47*, 3632.

[144] H. Gu, Y. Zhao, Y. Cheng, Z. Xie, F. Rong, J. Li, B. Wang, D. Fu, Z. Gu, *Small* **2013**, *9*, 2266.

[145] A. Loutfi, S. Coradeschi, G. K. Mani, P. Shankar, J. B. B. Rayappan, *J. Food Eng.* **2015**, *144*, 103.

[146] H. Zhu, J. Fan, B. Wang, X. Peng, *Chem. Soc. Rev.* **2015**, *44*, 4337.

[147] M. H. Lee, J. S. Kim, J. L. Sessler, *Chem. Soc. Rev.* **2015**, *44*, 4185.

[148] S. H. Foulger, P. Jiang, A. C. Lattam, D. W. Smith, J. Ballato, *Langmuir* **2001**, *17*, 6023.

[149] J. M. Jethmalani, W. T. Ford, *Chem. Mater.* **1996**, *8*, 2138.

[150] S. H. Foulger, P. Jiang, A. Lattam, D. W. Smith, J. Ballato, D. E. Dausch, S. Grego, B. R. Stoner, *Adv. Mater.* **2003**, *15*, 685.

[151] J. Ge, Y. Yin, *Angew. Chem.* **2011**, *123*, 1530.

[152] Z. Z. Gu, A. Fujishima, O. Sato, *J. Am. Chem. Soc.* **2000**, *122*, 12387.

[153] K. P. Raymond, I. B. Burgess, M. H. Kinney, M. Lončar, J. Aizenberg, *Lab Chip* **2012**, *12*, 3666.

[154] I. B. Burgess, N. Koay, K. P. Raymond, M. Kolle, M. Lončar, J. Aizenberg, *ACS Nano* **2012**, *6*, 1427.

[155] C. F. Blanford, R. C. Schroden, M. Al-Daous, A. Stein, *Adv. Mater.* **2001**, *13*, 26.

[156] S. Colodrero, M. Ocaña, H. Míguez, *Langmuir* **2008**, *24*, 4430.

[157] L. D. Bonifacio, D. P. Puzzo, S. Breslau, B. M. Willey, A. McGeer, G. A. Ozin, *Adv. Mater.* **2010**, *22*, 1351.

[158] A. C. Sharma, T. Jana, R. Kesavamoorthy, L. Shi, M. A. Virji, D. N. Finegold, S. A. Asher, *J. Am. Chem. Soc.* **2004**, *126*, 2971.

[159] D. Rus, M. T. Tolley, *Nature* **2015**, *521*, 467.

[160] J. Mu, G. Wang, H. Yan, H. Li, X. Wang, E. Gao, C. Hou, A. T. C. Pham, L. Wu, Q. Zhang, Y. Li, Z. Xu, Y. Guo, E. Reichmanis, H. Wang, M. Zhu, *Nat. Commun.* **2018**, *9*, 590.

[161] H. Xing, J. Li, Y. Shi, J. Guo, J. Wei, *ACS Appl. Mater. Interfaces* **2016**, *8*, 9440.

[162] S. Banisadr, J. Chen, *Sci. Rep.* **2017**, *7*, 1.

[163] W. Wei, Z. Zhang, J. Wei, X. Li, J. Guo, *Adv. Opt. Mater.* **2018**, *6*, 1800131.